Quaternary Research (2022), 1–26
doi:10.1017/qua.2022.8

Research Article

The Volchia Griva mineral oasis as unique locus for research of the mammoth fauna and the late Pleistocene environment in Northern Eurasia

Sergey V. Leshchinskiy[a,b]* and Elena M. Burkanova[a,b]

[a]Laboratory of Mesozoic and Cenozoic Continental Ecosystems, Tomsk State University, Lenin Ave. 36, Tomsk 634050, Russia. and [b]Sobolev Institute of Geology and Mineralogy, Siberian Branch of the Russian Academy of Sciences, Koptyug Avenue 3, Novosibirsk, 630090, Russia.

Abstract

This paper describes the results of research at Volchia Griva, the largest site in Asia containing mammoth fauna in situ. It is situated in the south of the West Siberian Plain in the Baraba forest-steppe zone, and occupies an area of several hectares. Analysis of sediments and taphonomy of the site allows us to suggest that thousands of megafaunal remains were buried here in mud pits and erosional depressions. The favorable geochemical landscape of Volchia Griva attracted animals during periods of mineral starvation. This is reflected in the high mortality in two intervals, ca. 20–18 ^{14}C ka BP and ca. 17–11 ^{14}C ka BP. The results of palynological analysis of samples from the upper part of the Volchia Griva section made it possible to reconstruct the history of landscape changes of the Baraba Lowland during the MIS 2. Forb-mesophytic meadows were common at the beginning of this period, with taiga type forests. At ca. 20 ^{14}C ka BP, an abrupt and significant aridization of the climate occurred, which led to the degradation of forests. The mammoth steppe was widely developed, dominated by forb-grass association and with areas of alkali meadows and soils. Such conditions existed probably until the mid-Holocene.

Keywords: Late Pleistocene, Western Siberia, Mammoth fauna, Paleoecology, Taphonomy, Paleogeography, Vegetation dynamics

(Received 17 May 2021; accepted 14 February 2022)

INTRODUCTION

The Volchia Griva (Wolf's Mound) site is well known among researchers of the Western Siberian Pleistocene. It is located in the southern part of the West Siberian Plain, in the Lake Chany closed basin. Currently, it is the largest mammoth "cemetery" (i.e., mass accumulation of remains) in Asia that was formed in situ. Geologists, paleontologists and archaeologists of the twentieth century studied the Volchia Griva (hereafter "VG") in 1957, 1967, 1968, 1975 and 1991. These studies made it possible to obtain a large amount of factual material, but the results of these campaigns were published as very preliminary findings. The calculation of the exact number of remains recovered during fieldwork is not possible due to the fragmentary and inconsistent information about the research conducted in the 1950s through 1970s. Nevertheless, analysis of all available data (including archival sources) allowed us to ascertain that the VG excavations in the twentieth century were carried out on an area of ~490–500 m^2. Within its limits, according to some sources, >5700 (or >7000, using other sources) fragments and whole bones and teeth from at least 70 woolly mammoths (*Mammuthus primigenius* Blum.), five horses, three bison, and one wolf were found, along with 37 lithic artifacts (Polunin, 1961; Zhylkibaev, 1963; Alexeeva and Vereshchagin, 1970; Okladnikov et al., 1971; Mashchenko and Leshchinskiy, 2001; Zenin, 2002).

Unfortunately, most of this unique faunal material discovered during the excavations of the twentieth century was subsequently lost or re-buried on the VG site. No more than 25% of the initial faunal material is preserved in collections of several institutions in Russia and Kazakhstan, including the composite skeleton of a subadult woolly mammoth mounted in 1960 at the Museum of Nature of the Institute of Zoology, Academy of Sciences of Kazakhstan. Such an attitude towards paleontological materials can be explained by the fact that the main efforts at that time were focused on the search for archaeological evidence of game-drive hunting of mammoths and finding dwellings made of bones and tusks. At the same time, at the beginning of the twenty-first century a ^{14}C age of ca. 18–11 ^{14}C ka BP was established using mammoth bones from the excavations of 1991 and test pits of 2000 and 2001 (Leshchinskiy et al., 2008).

In 2015, a new phase in the study of VG was launched, the trigger for which was the development of the geochemical hypothesis of the extinction of the woolly mammoth. It is based on the deep acidification of favorable Northern Eurasia geochemical landscapes at the end of the Pleistocene. Research shows that this led to chronic mineral starvation of animals and the formation of mammoth cemeteries around "beast solonetz" (salt or mineral licks), which served as mineral oases. In our opinion, the process of mammoth extinction in Northern Eurasia lasted for at least 20,000 years, and was largely caused by geochemical

*Corresponding author e-mail addresses: sl@ggf.tsu.ru, mammothfauna@gmail.com

Cite this article: Leshchinskiy SV, Burkanova EM (2022). The Volchia Griva mineral oasis as unique locus for research of the mammoth fauna and the late Pleistocene environment in Northern Eurasia. *Quaternary Research* 1–26. https://doi.org/10.1017/qua.2022.8

stress, clear manifestations of which were skeletal diseases (Leshchinskiy, 2009, 2012, 2015, 2017; Leshchinskiy et al., 2021a).

A large series of ^{14}C dates, obtained on mammal remains from the 2015–2018 VG excavations, confirmed the presence of the most southern and one of the youngest refugia of the mammoth fauna in Eurasia, which is located in the southern part of Western Siberia. This refugium existed for almost 10,000 years (since the last glacial maximum and possibly up to the Holocene), which is a unique phenomenon. Therefore, paleontological, stratigraphic, and paleoecological studies on the VG today focus on the comprehensive analysis of past ecosystems in the context of radical environmental changes in the Late Pleistocene.

PALEOECOLOGICAL CONTEXT

The problem of the extinction of the mammoth fauna and some of its species has been very important for >200 years (Cooper, 1831). The widespread distribution of Quaternary sediments and the application of advanced methods in their study today allow us to adequately reconstruct the dynamics of the extinction of the woolly mammoth, a key species of the late Pleistocene ecosystems in Northern Eurasia. One hundred thousand years ago, the range of the woolly mammoth covered almost the entire north of Eurasia, including the modern shelf zone of the North Atlantic, the Arctic Ocean, and the North Pacific, which was an uninterrupted body of land during the glaciations (Kahlke, 1999). However, at the end of the Pleistocene, the mammoth range shrunk rapidly. The main discussions are related to the time interval of ca. 24–9 ^{14}C ka BP, including the last glacial maximum and the late glacial period. A radiocarbon database for remains of mammoth and woolly rhinoceros recently became the basis for a model of megafaunal extinction, indicating a "retreat" to the north and northeast because dates younger than 12 ^{14}C ka BP are mainly known from the Siberian Arctic (Sulerzhitsky and Romanenko, 1997; Stuart et al., 2002, 2004).

According to recent data, the conclusion that the woolly mammoth became extinct before 12 ^{14}C ka BP in Western, Central, and Southern Europe is generally confirmed (Nadachowski et al., 2011, 2018; Ukkonen et al., 2011; Braun and Palombo, 2012). Nevertheless, today the mosaic nature of the mammoth range during its final stage of extinction on the continent at ca. 12–9 ^{14}C ka BP is clear. Most likely, viable mammoth populations still existed at that time in Eastern Europe, Western Siberia, Taimyr, Yakutia, and possibly in some other regions (Kuzmin, 2010; Puzachenko et al., 2017; Dehasque et al., 2021). Later on, mammoths continued to live on the islands of the Northern Pacific and Arctic oceans at ca. 5.7–3.7 ^{14}C ka BP (Vartanyan et al., 1995; Guthrie, 2004; El Adli et al., 2017). In Western Siberia, at least two mammoth refugia are known during MIS 2: (1) in the Konda Lowland and the Tura Plain, and (2) in the Baraba Lowland. In these areas, large mammoth fauna sites formed at Lugovskoe, Gary, and VG (Leshchinskiy et al., 2006, 2008; Chlachula and Serikov, 2010).

The Baraba Lowland is part of the West Siberian province of natron salt accumulation, where calcium, calcium-sodium, and sodium-hydroxyl geochemical landscapes are developed. Mineralization of natron water is maximal in the uppermost aquifers associated with Pleistocene deposits (Shvartsev, 1992, 1998). Salinization began in the Neogene, because at the beginning of the Pleistocene a large number of plant associations belong to species growing on alkali soils (Bukreyeva and Poleshchuk, 1970). Development of the geochemical landscapes of this territory at the end of the Pleistocene was expressed in the multiple salinization and desalinization of soils. The former is directly related to the evaporative concentration of elements coming to the surface from groundwater and, possibly, the addition of salts by atmospheric precipitation and dust from Central Asia. The main role in desalination was played by neotectonic uplift of the southern West Siberian Plain and humidification of the climate (Perelman, 1975).

The latest desalinization of landscapes in the forest-steppe zone of Western Siberia correlates with the general acidification of soils of Northern Eurasia clearly present after ca. 24 ^{14}C ka BP. This process probably led to the geochemical stress for mammoths, which is reflected by skeletal diseases (Leshchinskiy, 2006, 2009, 2012, 2015, 2017). Nevertheless, despite the degradation of Ca-Na geochemical landscapes as a whole, relatively favorable conditions for large herbivorous mammals existed in some parts of the Baraba Lowland at the very end of the Pleistocene and in the Early Holocene (Leshchinskiy, 2001; van der Plicht et al., 2015). The stability of ecological relationships and formation of the refugium in southern Western Siberia were due to the existence of mineral oases, and VG is a typical example of this. During mineral starvation, mammoths, horses, bison, and other megafaunal species were attracted to these areas. These foci of animal activity were certainly well known to ancient people who exploited the faunal remains (Leshchinskiy et al., 2008, 2015, 2021b).

REGIONAL SETTING

The VG site is situated in the eastern part of the Baraba Lowland (forest-steppe zone of Western Siberia). The generalized regional section shows sand and clay deposits with a total thickness of almost 3000 m (Babin et al., 2015). The mammoth "cemetery" is confined to the northeastern part of the eponymous sloping mound, elongated along the azimuth of ~50–55°. This mound is ~11 km long and ~0.5–1 km wide, with a maximal altitude of ~149 m (above the Baltic datum) and a relative elevation up to 15 m. The burial place is positioned within the boundaries of Mamontovoe (from the word "mammoth") Village, in Kargat County, Novosibirsk Province, Russia (Fig. 1). Manual exploratory drilling, digging of test pits, inspection of house cellars and water pipe trenches, and data from local residents allowed us to determine a total of at least several hectares where mammoth faunal remains were found.

MATERIALS AND METHODS

The data for this paper were collected from published and archival sources of the twentieth century, as well from the authors' descriptions of nine geological sections, >150 sediment and ground surface samples, >8 m of cores, documentation of excavations, and faunal and cultural remains obtained in 2015–2018. Excavations of the four field seasons within an area of ~38 m^2, with an almost complete collection of faunal materials (only very poorly preserved remains were not taken), yielded almost 2000 fragments and whole mammal bones and teeth. Altogether, 38 lithic artifacts also were recovered.

Descriptions of sections and taphonomic observations were accompanied by detailed photographing and sketching. The main emphasis was placed on the most accurate location of layers, proper sampling (especially with respect to the purity of samples), and careful positioning of sediment samples and paleontological

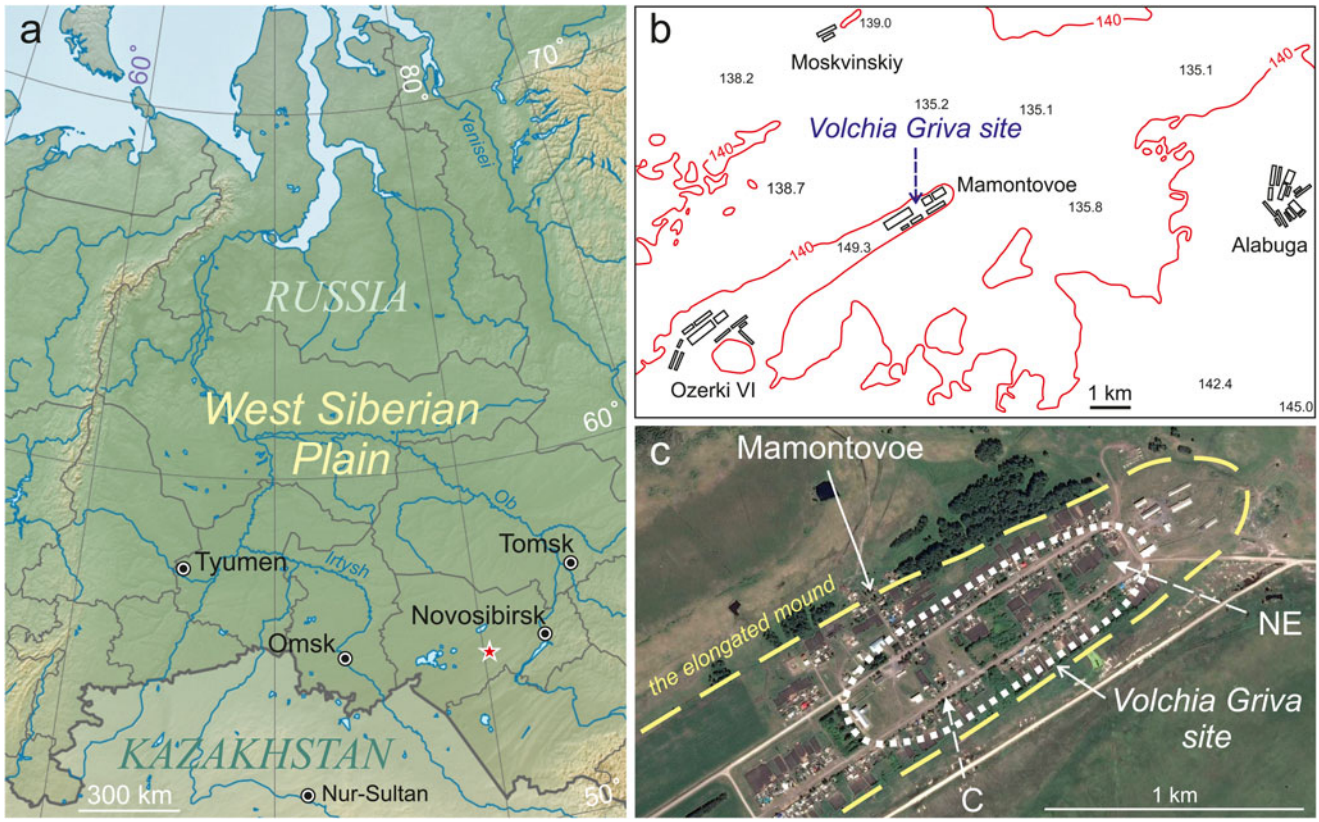

Figure 1. Position of the Volchia Griva: (**a**) administrative map of the West Siberian Plain (* indicates the site); (**b**) county map with local altitudes in meters; (**c**) the Volchia Griva site within Mamontovoe Village (satellite image), areas: C = central, NE = northeastern.

and archaeological finds with respect to certain elements of geological strata. Excavations were carried out following common modern practices. When cleaning of the bone-bearing horizon was undertaken, either layer-by-layer or by arbitrary levels (e.g., 0.5–5 cm inside thick strata), spatulas, brushes, and other small tools were used. The preparation of excavation plans (scale 1:20) was carried out using units in the form of 1 × 1 m grid size. The depth and spatial position of the remains were recorded using a surveyor's level and a compass. The entire volume of bone-bearing sediments was washed (sieves with a mesh of 1 × 1 mm), in order to recover bones and teeth of small vertebrates and tiny artifacts. The limits of the bone-bearing lenses and the peculiarities of the VG geological structure were clarified during borehole drilling. This work was carried out with a manual rotary-percussion drill (Eijkelkamp Co., Netherlands).

Post-mortem changes of bone surfaces were evaluated according to weathering stages 0–5 proposed by Behrensmeyer (1978). Individual ages and pathological skeletal changes were determined by comparison with materials on normal bone morphology and diseases of modern and Pleistocene large mammals, including humans (Logginov, 1890; Chepurov et al., 1955; Laws, 1966; Kovalskiy, 1974; Baryshnikov et al., 1977; Lang, 1980; Haynes, 1991; Rothschild et. al., 1994; Kuzmina and Maschenko, 1999; Lister, 1999; Maschenko, 2002; Rothschild and Martin, 2003; Rothschild and Laub, 2006, 2008; Johnson et al., 2007; Flueck and Smith-Flueck, 2008; Leshchinskiy, 2009, 2012, 2017; Clarke and Goodship, 2010; Lee et al., 2012; Krzemińska, 2014; Haynes and Klimowicz, 2015; Krzemińska and Wędzicha, 2015; Krzemińska et al., 2015).

Palynological analysis was performed at the Laboratory of Mesozoic and Cenozoic Continental Ecosystems, Tomsk State University (LMCCE TSU). Chemical treatment of samples was conducted at the Laboratory of Micropaleontology (LMP), TSU, in two ways: (1) sequential treatment by NaOH (20%) and HCl (10%), according to the standard procedure (Zaklinskaya and Panova, 1986); and (2) included treatment of the samples with $Na_4P_2O_7$, and then by HCl (10%). Demineralization in both cases was carried out by fractionation in a heavy liquid (density of 2.2 g/cm^3) based on a K-Cd mixture.

After treatment, pollen and spores were viewed using a Leica DM 1000 microscope with magnifications of 400, 630, and 1000. Atlases, published articles, and comparative collections of LMCCE and LMP were used to determine the taxonomy of pollen and spores. For each sample, at least 250 pollen grains usually were counted. Pollen spectra (PS) document the composition and ratio of individual seed plant taxa. The main percentage sum of each PS includes pollen of terrestrial plants: trees and shrubs (arboreal pollen "AP"), and herbs and dwarf shrubs (non-arboreal pollen "NAP"). Wetland and aquatic plant pollen (WAP), spores of seedless vascular plants, and non-pollen palynomorphs (NPP) were not taken into account, therefore their share was calculated from the sum of pollen of terrestrial plants. PS of similar taxonomic composition and ratios were combined into pollen complexes (PC).

The results of palynological analysis are presented in the form of tables and the pollen diagram for the upper part of the VG section. A detailed environmental reconstruction at the time of site formation was carried out by taking into account geological and taphonomic data.

Radiocarbon dating and stable isotope ratio ($\delta^{13}C$ and $\delta^{15}N$) analyses for the bone samples were conducted at the Center for Applied Isotope Studies, University of Georgia (Athens, GA, USA; lab code UGAMS). First, the bone was cleaned with a wire brush and washed in an ultrasonic bath. After physical cleaning, the dried bone was gently crushed into small fragments. The crushed bone was treated with 1N HCl at 4°C for 24 hours. The residue was filtered, treated with 0.1N NaOH in the filter to remove contamination caused by presence of humic acids, rinsed with deionized water, and under slightly acid condition (pH=3) heated at 80°C for six hours to dissolve collagen and leave humic substances in the precipitate. The collagen solution was then filtered to isolate the pure collagen and subsequently freeze-dried. The dried collagen was combusted at 575°C in an evacuated/sealed Pyrex ampoule in the presence of CuO. The resulting carbon dioxide was cryogenically purified from the other reaction products and catalytically converted to graphite using the method of Vogel et al. (1984). Graphite $^{14}C/^{13}C$ ratios were measured using the CAIS 0.5 MeV Accelerator Mass Spectrometer (AMS). The sample ratios were compared to the ratio measured from the Oxalic Acid I (NBS SRM 4990). The sample $^{13}C/^{12}C$ and $^{15}N/^{14}N$ ratios were measured separately using a stable isotope ratio mass spectrometer and expressed as $\delta^{13}C$ and $\delta^{15}N$ with respect to standards (PD belemnite and AIR, respectively), with an error of <0.1‰. The quoted uncalibrated ^{14}C dates have been given in radiocarbon years before AD 1950 (years BP), using the ^{14}C half-life of 5568 years. The error is quoted as one standard deviation and reflects both statistical and experimental errors. The ^{14}C dates have been corrected for isotope fractionation.

LOCATION AND ACCESSION OF PALEONTOLOGICAL MATERIALS

Paleontological materials from the 2015–2018 excavations are stored at the Laboratory of Mesozoic and Cenozoic Continental Ecosystems (LMCCE). Fieldwork, including the collection of faunal remains, was carried out by TSU based on license NOV 02790 PD, issued by the Department for Subsurface Use of the Siberian Federal District, Russian Federation.

RESULTS

We present here a summary of the results of paleontological, stratigraphic, taphonomic, and palynological studies conducted in the field and laboratory. The study and interpretation of extensive materials made it possible to better understand ecological aspects of the mammoth fauna, and to reconstruct environmental conditions during formation of the site. The emphasis here is on the 2015–2018 field campaigns. The fragmentary and inconsistent information from research conducted in the twentieth century and the incompleteness of the faunal collections obtained in those years do not allow their full use.

The resumption of multidisciplinary studies at VG occurred after almost a quarter-century break. An analysis of the available data shows that the bone-bearing horizon is not uniform laterally. It consists of a series of lenses traced over a distance of >1 km. Therefore, fieldwork was carried out in particular locations where the largest assemblages of mammoth faunal remains were identified—in the extreme northeastern part of VG, and in the center of Mamontovoe Village (Fig. 1).

The northeastern assemblage of mammoth fauna remains

The area with mammoth remains in the northeastern part of VG has been known since the 1950s. In the twentieth century, it was considered as the most promising part of the site, and all work was carried out here (Polunin, 1961; Alexeeva and Vereshchagin, 1970; Okladnikov et al., 1971; Mashchenko and Leshchinskiy, 2001). This information was decisive when research at VG was resumed in September 2015. The excavation pit, size of 4 × 3 m (WGS 84 coordinates: 54°40′01.9″N, 80°20′16.2″E; ground surface altitude ~147.3 m), oriented along magnetic azimuth of ~138°, is directly adjacent to the southwestern wall of the 1991 excavation pit No. 1. New excavations have shown that the remains of large mammals occur at a depth of 0.74–1.28 m below the ground surface (Figs. 2, 3). They are concentrated at the bottom of a loess-like loam with a compact (sometimes spotted) structure. The high content of carbonates is responsible for the very dense appearance of sediments at the bottom of the layer, and the loam ranges in color from gray-brown to white-gray (with greenish, dove-colored, or ashy shades). The bones at the bottom of this layer lie directly on thinly laminated, sandy clay sediments, which form the basis of the VG geological body. The bedding surface between the loess-like (bone-bearing) member and the underlying lacustrine-like (thinly laminated) member is clear—it is marked by cracks (mouths up to 5 cm wide) that penetrate as much as 0.6 m down the section.

In general, in the studied area, the bone-bearing horizon was represented by a subhorizontal body ~0.15–0.45 m thick, and many bones lie directly on top of each other. During the 2015 excavations, 611 remains of woolly mammoth and 20 remains of horses (*Equus* sp.) were recovered. If one accepts the average thickness of the bone-bearing horizon as ~0.3–0.35 m, the concentration of finds was more than 50 items/m^2. Taphonomic analysis indicates a high degree of bone weathering, which reaches a maximum in the arbitrary upper (Fig. 2) and middle levels of the bone-bearing horizon, where weathering stages 4 and 5 prevail. At the very bottom of the loess-like loam (arbitrary lower level), the bones have a less-weathered appearance (mainly stages 2 and 3) (Fig. 3). It is important to note that some more-weathered samples lie under less-weathered ones, which indicates possible post-depositional disturbance and interruptions in the formation of both the bone-bearing horizon and the matrix.

Minor subaerial sedimentation did not create conditions for the burial of whole carcasses. Therefore, animal remains could be completely destroyed in a few decades. This resulted in severe weathering and a high degree of bone fragmentation, their uneven distribution, and the rare occurrence of anatomical articulations (only four groups of vertebrae and a pes portion of mammoth, and a horse's metapodia were found). Better preservation at the bottom of the bone-bearing horizon can be explained by trampling of the mammoth bones and tusks into the moist clayey substrate by living mammoths and other large mammals. That is why the long bones are often crushed on their upper and lower sides. A steep dip (30° angle or more) of a part of the ribs and long bones at all levels indicates that they were trampled into the mud. Despite the fact that animal skeletons were exposed on the surface for a long time, gnawing marks by predators or scavengers are rare. Cut marks on bones that could have been left by ancient people were not recorded, although 48 lithic artifacts were found in the northeastern assemblage from all field seasons (Leshchinskiy et al., 2015, 2021b).

Figure 2. The arbitrary upper level of the VG bone-bearing horizon (2015 excavations). Weathering stages 4 and 5 of bone surfaces prevail. Solid arrows indicate long bones that were crushed during trampling; dashed arrow shows the mammoth pes portion.

The very high degree of weathering and trampling, as well as the activity of animals, including humans, resulted in the preservation of only few whole vertebrae, ribs, and long bones (mainly tibiae and radii) and their epiphyses, but many bones of manus and pes, and sesamoid bones, including patellae are present. Almost all remains have root traces, but it is impossible to prove that they are contemporaneous with the time of burial. The roots of modern plants penetrate into the loess-like loam and often entangle the bones. Many bones of the lower level are covered with a calcareous crust due to the high content of carbonates in the sediments. In general, most of the remains are represented by small fragments unsuitable for morphological studies. However, well-diagnosed large fragments and whole bones made it possible to establish that at least six woolly mammoths were present within the area excavated in 2015. Based on data of the dental stages and epiphysis fusion for long bones (Laws,

Figure 3. The arbitrary lower level of the VG bone-bearing horizon (2015 excavations). Weathering stages 2 and 3 of bone surfaces prevail. Broken ribs under pressure (solid arrows) and a steep dip of some bones (dashed arrows) indicate severe trampling.

1966; Haynes, 1991; Lister, 1999), it can be said that two of individuals were >25 years old when they died, one was 12–25 years old, and two were <12 years old. One individual was a calf up to one year old, possibly a newborn or fetus, as evinced by the atlas fragment with unfused left and right parts of the dorsal arch (Maschenko, 2002). Horse remains are found only in the lower level, and consist of at least two individuals about two years old.

Paleontological materials obtained in 2015 were used to clarify the age of the VG northeastern assemblage. Previously, the period of its formation was estimated in the range of ca. 18–11 ^{14}C ka BP (Leshchinskiy et al., 2008). More recently, new AMS radiocarbon dates were produced, the oldest three values of which are from the base of the bone-bearing horizon. Two of them, obtained from the upper and lower jaws of horses from depths of 1.14–1.2 m and 1.07–1.1 m, respectively, gave ages of 19,130 ± 50 ^{14}C yr BP (UGAMS-26104) and 18,840 ± 50 ^{14}C yr BP (UGAMS-26107). The third value of 18,840 ± 50 ^{14}C yr BP (UGAMS-26110) was obtained from a tusk found at a depth of 1.1–1.16 m. The youngest date, 17,840 ± 60 ^{14}C yr BP (UGAMS-26111), belongs to a mammoth pelvis from a depth of 0.74–0.99 m (Table 1). It is impossible to determine the exact stratigraphic position of this find, because the boundary between the bone-bearing levels in this part of VG is unclear. Nevertheless, it is now clear that the burial process of the megafauna here began earlier than 19 ^{14}C ka BP.

The central assemblage of mammoth fauna remains

In 2016–2018, studies were carried out on a previously unexplored area in the center of Mamontovoe Village, ~700 m from the twentieth century and 2015 excavations. In 2016, an excavation pit of 3 × 3 m was set up on Molodezhnaya Street, between house no. 35 and the roadway (WGS 84 coordinates: 54° 39′48.4″N, 80°19′47.6″E; ground surface altitude ~148 m). The walls of the pit are oriented along magnetic azimuths of ~46° and 136°. Fieldwork results show that the upper bone-bearing level here is practically absent, and only a single fragment of a bison's mandible, which was found at a depth of 0.86–0.9 m, can be preliminarily assigned to it. Farther below, at a depth of 1.04–1.47 m (an average interval of 1.2–1.4 m), a typical bone-bearing lens was excavated (Fig. 4), with 207 remains—almost all from mammoths, including the manus portion in anatomical position (Fig. 4b). The degree of bone weathering (stages 1–5) and surrounding subaerial sediments generally correspond to the information available from both taphonomy and geology of the northeastern part of VG.

However, below the interval of ~0.15–0.3 m thick, a bone-bearing level was also revealed, which was not previously noted. At a depth of ~1.55–2.15 m (average interval 1.65–2.1 m), fragments and whole vertebrae, scapulae, ribs, skull bones, and limbs of calves and adult mammoths with a concentration of ~100 items/m^2 were found. These remains are very well preserved (weathering stages 0 and 1 prevail), because they were quickly sealed by sandy clay material in the upper part of a small gully ~1.6 m deep and >4 m wide. This also explains the relatively large number of anatomical articulations (Fig. 5). It is noteworthy that a large mandible, fused ulna, and radius were found higher in the section (the bone tops at a depth of ~1.45–1.47 m), which led to greater weathering of their surfaces. In the center of this assemblage, many bones lie on top of each other, which caused indentations. Some bones are positioned at steep angles, and a large tusk (alveolus diameter of ~15 cm) penetrated the lower level to its bottom.

The unique taphonomy of the central assemblage led to the highest degree of concentration of finds in the main part of the 2016 excavation pit, >130 items/m^2 (~3 m^2 of excavated space were without finds). In total, 792 mammal remains, including fragments, were found. Almost all of them belong to at least eight mammoths: from adults to 0–2 years old, and possibly fetuses. The small sizes of ribs and long bones, which demonstrate the early stages of ontogenesis, indicate the ages (Maschenko, 2002; Fisher et al., 2014). It is important to note that mammoth bones represent all divisions of the skeleton, and the bones in the lower level are significantly larger than analogous bones in the middle level that belong to individuals of similar age. This conclusion was made on the basis of the described process of epiphyseal fusion in the mammoth's long bones (Lister, 1999). Noteworthy among the large bones of the lower level is a femur with fused epiphyses ~1.15 m long that most likely belongs to a male older than 45 years. This individual could have weighed 5–6 tons, with a calculated height of >3 m (Christiansen, 2004; Larramendi, 2016). Only 38 remains, or a few more (some fragments cannot be identified up to species), belong to other taxa. Among large mammals, there are bones and teeth of bison (*Bison* sp.); horse (*Equus* sp.; anatomical articulation of the three phalanges and sesamoid bone of an individual <1.5 years old); bear (*Ursus* sp.; one tooth), and apparently wolf (*Canis* sp.; scapula and pelvis fragments of two individuals). For the first time, rodents and medium-sized carnivores (foxes) were found in the bone-bearing horizon of the VG. Similar morphology and disunity of the remains (fragments of mandible and skull, and teeth) do not allow us to confidently identify them to the species level: it is either polar fox (*Vulpes lagopus* L.) or red fox (*V. vulpes* L.).

In 2017, excavations were carried out in an area of 3 × 3 m, directly adjacent to the 2016 pit, between house no. 35 on Molodezhnaya Street and the roadway. As a result, the remaining transverse part of the aforementioned gully was excavated. Six poorly preserved bone fragments were assigned to the upper and middle levels in the interval of 0.96–1.26 m. The lower bone-bearing level was determined in a narrow strip of ~2 m^2, at a maximum depth of 2.04 m (Fig. 6). One hundred mammal remains

Table 1. The results of radiocarbon analysis for the samples from the northeastern assemblage of the Volchia Griva site (2015 excavation).

Laboratory No.	Sample field No.	^{14}C yr BP	Material	Depth from surface, m	Bone-bearing levels
UGAMS-26104	591	19,130 ± 50	horse bone	1.14–1.20	base of the lower
UGAMS-26107	331	18,840 ± 50	horse bone	1.07–1.10	base of the lower
UGAMS-26110	403	18,840 ± 50	mammoth tusk	1.10–1.16	base of the lower
UGAMS-26111	4	17,840 ± 60	mammoth bone	0.74–0.99	uncertain

Figure 4. The middle level of the VG bone-bearing horizon (2016 excavations). Weathering stages of bone surfaces present are from 1–5. Solid arrows indicate long bones and the pelvis (**a**) with the highest degree of weathering; dashed arrows show portions of the vertebral column and mammoth manus (**b**) in anatomical position.

were recovered, 95 of which belong to mammoth (apparently, to those individuals found in 2016). Other remains belong to horse; probably, polar fox; and rodents. The weathering of bone surfaces is identical to that found during the 2016 excavations.

Well-chosen excavation areas in 2016–2017 allowed us to re-open the part of the ancient small gully with the bone-bearing horizon of the central faunal assemblage. Description of stratigraphy with sampling for laboratory studies formed the basis for a summary cross-section of this erosional form, which clearly was expressed on the southeastern walls of 2016–2017 pits (Fig. 7).

In 2018, a 4 × 2 m excavation pit was laid 11 m from the 2016–2017 excavations (in the magnetic azimuth of 315°) on the other side of the roadway, in front of house no. 18 on Molodezhnaya Street. The long wall of the pit is oriented along the magnetic azimuth of 45° (along the street). The upper level of the bone-bearing horizon was absent. In the middle level, 160 remains were found, almost all of them belonging to mammoths (Fig. 8, 9a). Weathering of bone surfaces in most cases reaches stages 3–5. Bone sizes indicate a minimum of two mammoths (immature and young adult). Extraordinary finds include the manus

Figure 5. The lower level (upper part) of the VG bone-bearing horizon (2016 excavations). Remains of at least three mammoths are visible. Weathering stages 0 and 1 of bone surfaces prevail. Solid arrows indicate anatomical articulations of the vertebrae; dashed arrows show the fused ulna and radius, the large mandible lying above the rest of bones; (**a**) humerus with strong gnawing marks (dotted arrows); (**b**) the tusk distal end penetrates down to the bottom of horizon (contoured by dashed lines); dotted arrow indicates mammoth spinous process with a hole (pathology).

portion and 20 vertebrae in anatomical position (Fig. 8a, b). Only one fragment of the mandible belongs probably to the polar fox (Fig. 8d), and the species for several fragments were not identified due to poor preservation. The depth of occurrence for remains in the middle level was in the range 0.52–1.06 m. A rather large interval is associated with a significant drop in sediment depth towards the ancient gully. In addition, trampling of bones played a significant role in their vertical distribution. This is clearly demonstrated by the mammoth rib from a depth of 0.68–1.12 m, the distal end of which stood vertically in the middle level, and the proximal end was immersed into the lower level (Fig. 8c).

The lower bone-bearing level lies almost immediately below the middle one at a depth of 0.91–1.37 m. The finds are a continuation of the assemblage in the ancient gully that was excavated in 2016–2017. Its boundary is clearly seen by a sharp decrease in the paleo-microrelief (Fig. 9). Quick burial of bones in sandy clay, likely of colluvial and coastal-lacustrine genesis, determined the predominance of weathering stages 0–1. Nevertheless, remains of stage 5 are also found here, which indicates re-deposition or trampling. Almost all of the total 280 mammal remains found in the lower level of 2018 belong to mammoths. An important find is portions of a maxilla with dP^2 and dP^3. The absence of occlusal wear on the teeth, their small sizes, and other signs

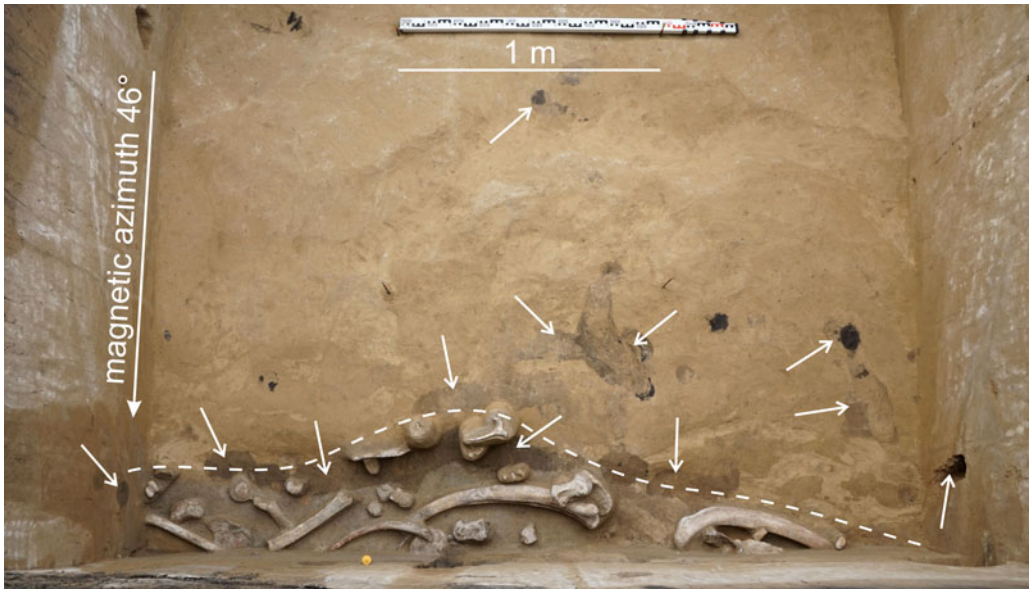

Figure 6. The bottom of the VG bone-bearing horizon (2017 excavations). The gully limit is clearly visible (contoured by dashed line). Solid arrows indicate numerous holes of burrowing animals.

(Roth and Shoshani, 1988; Rountrey et al., 2012) indicate that these remains belong to a fetus. Other taxa are represented by horse (hoof phalanx and sesamoideum), and probably polar fox (portions of the skull and a mandible).

The bone-bearing horizon in all the excavations was disturbed by the holes of burrowing animals. In the lower level, the holes sometimes remained hollow when they are located under large bones (Figs. 6, 9). These biogenic disturbances appear to be of Holocene age. Given the frequent death of rodents in these holes, and perhaps sometimes of small carnivores, there is a possibility of mixture of remains of different ages. To minimize this negative factor, the fillings of holes were excavated and washed separately (Fig. 10). As a result, numerous bones and teeth of several rodent species with excellent preservation were found, which were taken into account separately.

Along with the mammoth fauna remains in the central assemblage, lithic artifacts were also found (eight items in 2016; four in 2017; 15 in 2018). Artifacts are associated mainly with the lower bone-bearing level (Leshchinskiy et al., 2021b), which indicates that Paleolithic humans were present at VG already at the early stage of the site's formation.

The age of remains from the VG central assemblage before the 2015–2018 campaigns was unknown. A series of AMS ^{14}C dates showed that a bone-bearing horizon here began to form almost immediately after 20 ^{14}C ka BP, and this process continued practically until the end of the Pleistocene. Thus, burial of remains occurred synchronously throughout the whole explored VG area. The distribution of dates by bone-bearing levels is shown in Table 2.

Based on the 2016 data, the seven oldest dates for the lower level are in the range of ca. 19.6–19.1 ^{14}C ka BP. Four of these values were run on horse (first phalanx; depth of 1.91–1.95 m), wolves (pelvis and scapula fragments; depths of 1.62–1.65 m and 1.87–1.88 m, respectively), and the polar/red fox (skull fragments; depth of 1.90–1.91 m). The rest of the dates come from mammoths: a fragment of a tusk alveolus from a depth of 1.97–2.05 m; and the spinous processes of the vertebrae with holes (pathology) from depths of 1.69–1.76 m and 1.77–1.83 m. The youngest date for the lower level is 18,420 ± 45 ^{14}C yr BP (UGAMS-32278), obtained on a mammoth scapula from a depth of 1.58–1.79 m. The middle bone-bearing level in the 2016 excavation pit was clearly separated from the lower one, but its oldest date is 18,460 ± 45 ^{14}C yr BP (UGAMS-32277) (on a mammoth femur from a depth of 1.24–1.42 m), which overlaps with the age of the lower level. The youngest date of the middle level is 13,700 ± 35 ^{14}C yr BP (UGAMS-32275) on the mammoth pelvis from a depth of 1.04–1.38 m. The date of the bison bone from the arbitrary upper level is 16,750 ± 45 ^{14}C yr BP (UGAMS-32286).

Dates obtained from the 2017–2018 excavations clarify the age of the middle bone-bearing level. The spinous process of the vertebra and a fragment of the mammoth bone, found in 2017 at depths of 1.11–1.15 and 0.97–1.03 m, are dated to 16,550 ± 40 ^{14}C yr BP (UGAMS-32282) and 15,870 ± 40 ^{14}C yr BP (UGAMS-32281), respectively. The mammoth ulna and humerus, found in 2018 at depths of 0.74–0.94 and 0.73–0.93 m, are dated to 18,640 ± 40 ^{14}C yr BP (UGAMS-40949) and 10,620 ± 30 ^{14}C yr BP (UGAMS-40948), respectively (Table 2).

The boundaries of the central faunal assemblage were determined by drilling 60 boreholes (without sampling). As a result, it was found that the bone-bearing lens covers an area of >350 m^2, with a maximum depth of remains at >3.5 m. In addition, two boreholes (with sampling of 95% of the core's length) were drilled at the foot of VG to clarify the summary geological section.

When we characterize the results of the fieldwork, it is important to note pathological changes on the mammoth bones found in 2015–2018. Moreover, they are recorded at all levels of the bone-bearing horizon in both assemblages. It should be recalled that a correct paleopathological analysis of the faunal materials collected at the VG site during the twentieth century excavations is impossible because of fragmentation and separation. However, in these collections, skeletal and dental abnormalities are also noted (Maschenko and Leshchinskiy, 2001; Shpansky, 2014). A high degree of weathering and fragmentation of the remains

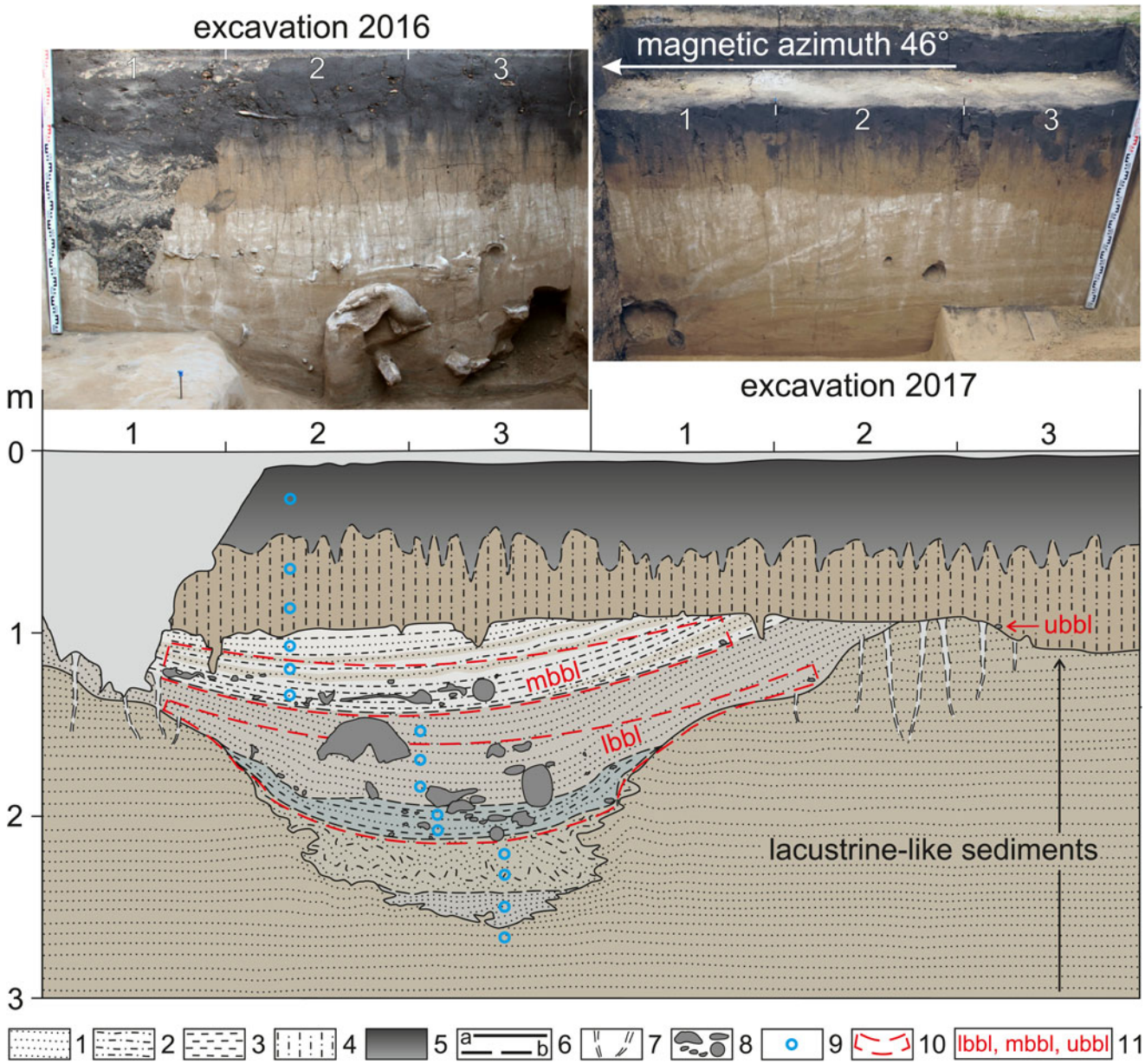

Figure 7. Cross-section of the ancient small gully with bone-bearing horizon of the VG central faunal assemblage. 1 = sand; 2 = silt; 3 = clay; 4 = loess-like loam; 5 = soil; 6 = boundaries: a, certain; b, assumed; 7 = desiccation cracks; 8 = faunal remains; 9 = sampling points; 10 = boundaries of bone-bearing levels; 11 = bone-bearing levels: lbbl, lower bone-bearing level; mbbl, middle bone-bearing level; ubbl, upper bone-bearing level.

makes the diagnosis of the skeletal diseases more complicated. However, exostoses, osteolysis, and peripheral erosion of the articular surfaces are clearly identified. Controversial destructions in the form of holes in the spinous processes of the vertebrae were also found (Figs. 5, 11). In general, this is usually a sign of osteodystrophy, which often develops due to a deficiency of vital macro- and microelements in the environment and, concomitantly, in forage and drinking water (Chepurov et al., 1955; Kovalskiy, 1974; Leshchinskiy, 2015; Leshchinskiy et al., 2021a).

Data on stable isotopes for bone collagen samples obtained from the central faunal assemblage (Table 2) indicate biogeochemical characteristics of the VG mammal diet. The atomic C/N ratios of the collagen for all samples (except one) are within the range of 2.9–3.6, which is recommended for reliable data (Ambrose, 1990; Guiry and Szpak, 2021). The $\delta^{13}C$ and $\delta^{15}N$ values of mammal bone samples are plotted relative to time (Figs. 12 and 13, respectively). The $\delta^{13}C$ value range for mammoths is from −21.40‰ to −20.01‰, with an average of −20.56‰; for carnivores from −18.82‰ to −16.89‰, with an average of −18.00‰; the value for horse is −19.16‰, and for bison −19.23‰. The $\delta^{15}N$ values for mammoths are from 7.90‰ to 14.67‰, with an average of 12.90‰; for carnivores from 16.20‰ to 17.10‰, with an average of 16.60‰; and values for horse and bison are 12.32‰ and 4.76‰, respectively.

Palynological research

Subaerial deposits are often characterized by a low concentration of plant remains, particularly pollen and spores. Basically, this is due to the slow rate of aeolian and colluvial sedimentation, which

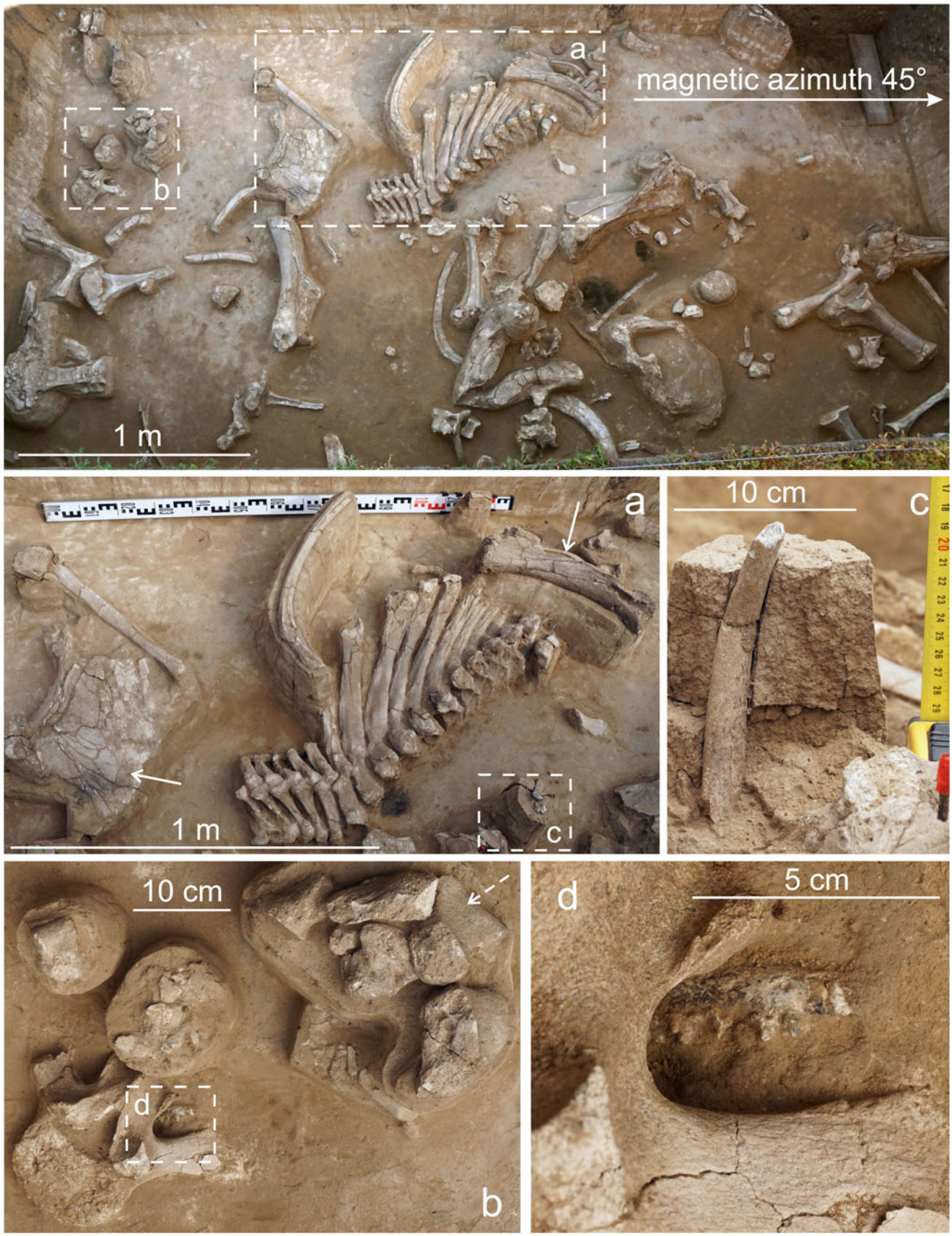

Figure 8. The middle level of the VG bone-bearing horizon (2018 excavations). Remains of at least two mammoths are visible. Weathering stages 3–5 of bone surfaces prevail. (**a**) Large portion of vertebral column in anatomical position, solid arrows indicate the pelvis fragment and the humerus with highest weathering; (**b**) manus portion in anatomical position (dashed arrow); (**c**) vertical rib position indicating severe trampling; (**d**) fox mandible fragment under mammoth lumbar vertebra.

Figure 9. Structure of the VG bone-bearing horizon at the central faunal assemblage (2018 excavations). (**a**) middle level, (**b**) upper part of the lower level, (**c**) bottom of the lower level. Dashed lines show change of the ancient gully/mud pit limits. Solid arrows indicate holes of burrowing animals.

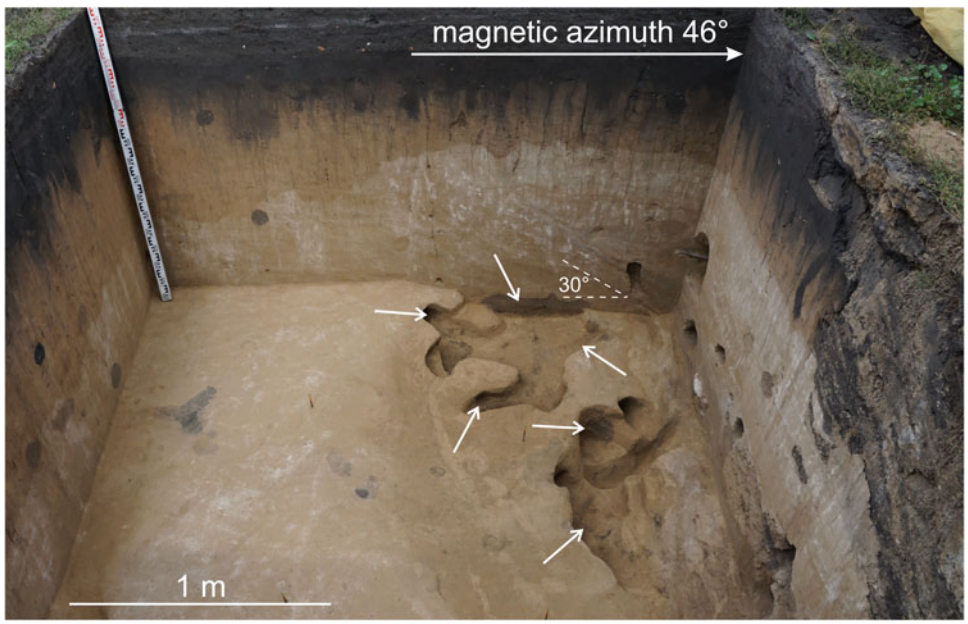

Figure 10. Holes of burrowing animals (solid arrows) that were excavated and washed separately (2017 excavations). Note the steep dip (angle up to 30° or more) of sediments in the cross-section of the ancient gully.

leads to long exposure of microfossils on the ground surface. Weathering and other geological processes contribute to the rapid destruction of pollen and spores, as well as to their transport and re-deposition. Loess-like deposits prevail in the upper part of the VG profile; therefore, samples for palynological analysis were collected from the cross-section of the ancient small gully along the southeastern wall of the 2016 excavation pit (Fig. 7). In this local erosional site, the bone-bearing lens of the central faunal

Table 2. The results of radiocarbon and isotopic analyses for the samples from the central assemblage of the Volchia Griva site (2016–2018 excavations).

Laboratory No.	Sample field No.	^{14}C yr BP	δ^{13}C, ‰	δ^{15}N, ‰	Material dated	Depth from surface, m	Bone-bearing levels (excavation year)
UGAMS-32287	674	19,540 ± 50	−19.16	12.32	horse bone	1.91–1.95	lower (2016)
UGAMS-32284	251	19,450 ± 50	−16.89	16.48	wolf bone	1.62–1.65	lower (2016)
UGAMS-32272	550	19,360 ± 50	−18.28	16.20	fox bone	1.90–1.91	lower (2016)
UGAMS-32288	468	19,320 ± 50	−20.14	13.12	mammoth bone (with pathology)	1.77–1.83	lower (2016)
UGAMS-32273	619	19,250 ± 50	−18.82	17.10	wolf bone	1.87–1.88	lower (2016)
UGAMS-32283	719	19,240 ± 50	−20.81	14.67	mammoth bone	1.97–2.05	lower (2016)
UGAMS-32289	237	19,160 ± 50	−20.21	13.05	mammoth bone (with pathology)	1.69–1.76	lower (2016)
UGAMS-32278	272	18,420 ± 45	−20.37	12.86	mammoth bone	1.58–1.79	lower (2016)
UGAMS-40949	7	18,640 ± 40	−20.01	13.45	mammoth bone	0.74–0.94	middle (2018)
UGAMS-32277	46	18,460 ± 45	−20.61	13.20	mammoth bone	1.24–1.42	middle (2016)
UGAMS-32282	7	16,550 ± 40	−20.53	13.65	mammoth bone	1.11–1.15	middle (2017)
UGAMS-32281	3	15,870 ± 40	−20.34	13.24	mammoth bone	0.97–1.03	middle (2017)
UGAMS-32275	146	13,700 ± 35	−21.40	7.90	mammoth bone	1.04–1.38	middle (2016)
UGAMS-40948	110	10,620 ± 30	−21.18	13.84	mammoth bone	0.73–0.93	middle (2018)
UGAMS-32286	1	16,750 ± 45	−19.23	4.76	bison bone	0.86–0.90	upper? (2016)

Figure 11. Mammoth vertebra with a hole in the spinous process (2016 excavations).

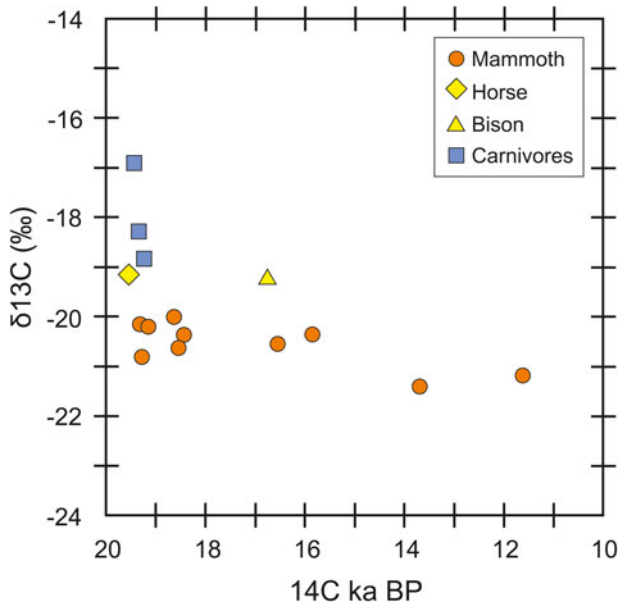

Figure 12. δ^{13}C values of VG mammal bone collagen through time.

assemblage was relatively quickly buried, probably by colluvial and coastal-lacustrine material.

Comparison with recent pollen spectra (PSs) was carried out on four samples (A, B, C, D) collected from the ground surface to a depth of as much as 1 cm. Different areas and plant associations were chosen for this: A and B—at the top of the VG mound, near the 2015 excavation pit and the birch forest outlier; C and D—at the foot of the VG mound, on the dry and boggy areas, respectively.

Laboratory preparation of the samples allowed retrieval of pollen and spores in sufficient quantities for statistical processing. Fragments of plant tissues, charcoal, and mineral particles were also found in all samples. Statistics on the results of palynological analysis are presented in Tables 3–5, and a pollen diagram in Figure 14.

In the upper part of the VG section, including the bone-bearing horizon and underlying and overlapping sediments, three PCs are distinguished from bottom to top. In the first PC, tree pollen represents a significant part; in the second and third PCs, herb pollen prevails; their detailed descriptions are presented below.

PC1 characterizes the top of lacustrine-like sediments of the main body of VG and probably two subaerial layers underlying the bone-bearing horizon. Changes in the percentage of taxa made it possible to divide PC1 into three sub-complexes: PC1a, PC1b, and PC1c (Table 3; Fig. 14).

PC1a (PS of sample 1) and PC1c (PSs of samples 3, 4) are very similar to each other. The AP is 44.9–52.1% of the main percentage sum, dominated by *Pinus* spp. and *Picea* sp. *Betula* sp. also is

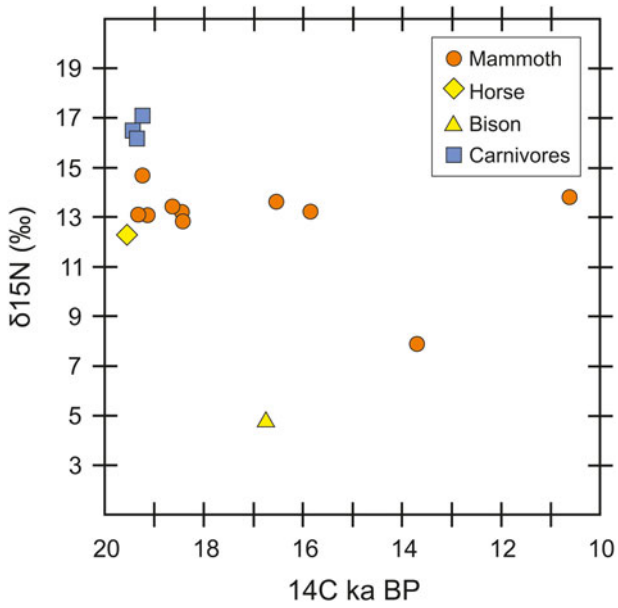

Figure 13. $\delta^{15}N$ values of VG mammal bone collagen through time.

constantly present, and more rarely, *Abies* sp. and *Salix* sp. About 25% of the main percentage sum in the NAP group belongs to Tricolpopollenites (three-furrow pollen with an unclear morpho-sculpture). In addition, pollen of Asteraceae, Chenopodiaceae, Poaceae, and other forbs (Rosaceae, Caryophillaceae, Cichoriaceae, Brassicaceae, Lamiaceae, Ranunculaceae, Valerianaceae) are present. The WAP (Cyperaceae, *Potamogeton* sp., *Typha* sp.) is constantly present, with its content of 4.7–11.4% of AP + NAP. Rare spores belong to *Equisetum* sp., *Sphagnum* sp., and ferns with Monoletes-type spores. The NPPs are represented by large numbers of *Pediastrum* sp. algae, and by rare fruit bodies of *Glomus* sp. fungi.

PC1b (PS sample 2) lies between the PC1a and the PC1c. It is characterized by an identical taxonomic composition of trees and herbs. The difference lies in the AP content, which drops to 25.1% of the main percentage sum, mainly due to an increase in the amount of Tricolpopollenites (46.4%). The WAP (Cyperaceae, *Potamogeton* sp.) accounts for 4.3% of AP + NAP. Rare spores belong to *Sphagnum* sp. and ferns with Monoletes-type spores. The NPPs are also represented by a large amount of *Pediastrum* sp. algae, and by rare fruit bodies of *Glomus* sp. fungi.

PC2 characterizes the lower and middle bone-bearing levels (sediments in the ancient gully) and the overlying subaerial sediments. In all PSs, the NAP is clearly dominant (80.6–98.1% of the main percentage sum). Changes in the percentage of individual taxa made it possible to divide PC2 into six sub-complexes: PC2a, PC2b, PC2c, PC2d, PC2e, and PC2f (Tables 3, 4; Fig. 14).

PC2a (PS of sample 5) reflects the very bottom of the bone-bearing horizon. The AP constitutes 14% of the main percentage sum, and this group is represented mainly by *Pinus* spp. The content of *Picea* sp. pollen is 3.9%. Therefore, the amount of NAP is 86%, dominated by Tricolpopollenites (40.1%), and sharply increased Poaceae (15.1%) and *Artemisia* sp. (7.9%). *Ephedra* sp. is also present. Other NAP includes forbs: Rosaceae, Brassicaceae, Scrophulariaceae, Cichoriaceae, Caryophillaceae, and Ranunculaceae. The WAP (Cyperaceae gen. indet. and *Potamogeton* sp.) constitutes 1.8% of AP + NAP. Very rare spores belong to *Equisetum* sp. and *Sphagnum* sp. NPPs are represented by rare remains of *Pediastrum* sp. algae, a large number of fruit bodies of *Glomus* sp. fungi, and hyphae and spores of unidentified fungal taxa.

PC2b (PS of sample 6) belongs to the lower bone-bearing level. The AP content is minimal for PC2 and amounts to 1.9% of the main percentage sum. This group is represented mainly by deformed and fragmented pollen of Pinaceae gen. indet., while pollen of *Picea* spp. and *Betula* sp. occur in very small quantities. The amount of NAP is 98.1%, and >58% belong to Tricolpopollenites and *Artemisia* sp. The content of Poaceae does not exceed 3.9%. Other NAPs include Rosaceae, Brassicaceae, Cichoriaceae, Caryophillaceae, and Ranunculaceae. Pollen of Chenopodiaceae, *Ephedra* sp., and WAP, and spores are absent. The NPPs consist of a large number of fruit bodies of *Glomus* sp. fungi, and hyphae and spores of unidentified fungal taxa.

PC2c (PSs of samples 7, 8) characterizes sediments of the main part of the lower bone-bearing level. The AP content is 6.5–6.7% of the main percentage sum. *Pinus* spp. predominates, including deformed and fragmented pollen of Pinaceae gen. indet. The NAP (93.3–93.5%) contains mainly Tricolpopollenites and Asteraceae, including *Artemisia* sp., with *Ephedra* sp. also present. Other NAP taxa are Caryophillaceae, Cichoriaceae, Fabaceae, Scrophulariaceae, Rosaceae, Brassicaceae, Ranunculaceae, Polygonaceae, Valerianaceae, and Primulaceae, including Plumbaginaceae with Limonium-type pollen. The PSs of this interval contain WAP (Cyperaceae, *Potamogeton* sp.), up to 3.9% of AP + NAP. The NPPs have large numbers of fruit bodies of *Glomus* sp. fungi, and hyphae and spores of unidentified fungal taxa, and phytoliths.

PC2d (PS of sample 9) is associated with sediments between the lower and middle bone-bearing levels. The AP content increases to 19.4% of the main percentage sum. Pollen of *Pinus* s/g Diploxylon predominates. Pollen of *Betula* sp. and Pinaceae gen. indet. is present in approximately equal amounts. The NAP (80.6%) is mainly represented by Tricolpopollenites, Chenopodiaceae, and Asteraceae including *Artemisia* sp. Pollen of *Ephedra* sp. is also present. Other NAP taxa are Caryophillaceae, Scrophulariaceae, Lamiaceae, Rosaceae, Brassicaceae, Ranunculaceae, and Polygonaceae. The content of WAP (Cyperaceae and *Potamogeton* sp.) increases to 7% of AP + NAP. The NPPs include a large number of fruit bodies of *Glomus* sp. fungi, and hyphae and spores of unidentified fungal taxa, and phytoliths.

PC2e (PSs of samples 10, 11) characterizes sediments of the middle bone-bearing level. The AP content is 6.3–7.5% of the main percentage sum. Deformed and fragmented pollen of Pinaceae gen. indet. predominates. *Pinus* s/g Diploxylon, *Betula* sp., *Populus* sp., and *Salix* sp. are constantly present. The NAP (92.5–93.7%) is characterized mainly by Tricolpopollenites (up to 40.1%). Increased content of Chenopodiaceae (up to 11.9%) is typical for this interval. Pollen of *Ephedra* sp. is absent. Other NAP taxa are Caryophillaceae, Cichoriaceae, Lamiaceae, Scrophulariaceae, Rosaceae, Brassicaceae, Ranunculaceae, Polygonaceae, and Silenaceae. The content of WAP is 1.6–2.2% of AP + NAP. NPPs are presented by a large quantity of fruit bodies of *Glomus* sp. fungi, and hyphae and spores of unidentified fungal taxa.

PC2f (PS of sample 12) likely characterizes the aeolian-colluvial sediments that overlap the middle bone-bearing level. The AP content (Pinaceae gen. indet., *Betula* sp.) is 4,7% of the main percentage sum. The NAP (95.3%) is represented mainly

Table 3. Number and share of pollen grains and spores in samples 1–6 (AP and NAP as% of the main percentage sum, WAP and spores as % of AP+NAP). Abbreviations to Tables 3–5 and Figure 14: AP = arboreal pollen, NAP = non-arboreal pollen, WAP = wetland and aquatic plant pollen.

Taxonomic composition	1	%	2	%	3	%	4	%	5	%	6	%
AP	**196**	**51.9**	**165**	**25.1**	**263**	**44.9**	**99**	**52.1**	**39**	**14.0**	**5**	**1.9**
Abies sp.	2	0.5	1	0.2	8	1.4						
Picea sp.	35	9.3	33	5.0	33	5.6	11	5.8	11	3.9	1	0.4
Pinaceae gen. indet.	56	14.8	43	6.5	70	11.9	7	3.7	12	4.3	3	1.2
Pinus s/g Diploxylon	77	20.4	58	8.8	108	18.4	47	24.7	10	3.6		
Pinus s/g Haploxylon	17	4.5	9	1.4	12	2.0	22	11.6	4	1.4		
Betula sp.	9	2.4	19	2.9	29	4.9	10	5.3			1	0.4
Populus sp.							1	0.5	1	0.4		
Salicaceae gen. indet.			2	0.3	3	0.5	1	0.5	1	0.4		
NAP	**182**	**48.1**	**492**	**74.9**	**323**	**55.1**	**91**	**47.9**	**240**	**86.0**	**252**	**98.1**
Ericaceae gen. indet.					1	0.2						
Ephedra sp.					1	0.2	1	0.5	1	0.4		
Asteraceae gen. indet.	23	6.1	29	4.4	25	4.3	13	6.8	13	4.7	4	1.6
Artemisia sp.	13	3.4	9	1.4	18	3.1	3	1.6	22	7.9	16	6.2
Chenopodiaceae gen. indet.	23	6.1	66	10.0	42	7.2	7	3.7	3	1.1		
Poaceae gen. indet.			3	0.5	9	1.5			42	15.1	10	3.9
Tricolpopollenites	82	21.7	305	46.4	143	24.4	47	24.7	112	40.1	138	53.7
Other	41	10.8	80	12.2	84	14.3	20	10.5	47	16.8	84	32.7
Total (AP+NAP)	**378**	**100**	**657**	**100**	**586**	**100**	**190**	**100**	**279**	**100**	**257**	**100**
WAP	**25**	**6.6**	**28**	**4.3**	**67**	**11.4**	**9**	**4.7**	**5**	**1.8**		
Cyperaceae gen. indet.	1		12		17		2		4			
Potamogeton sp.	24		16		48		7		1			
Sparganium sp.					1							
Typha sp.					1							
Spores	**7**	**1.9**	**3**	**0.5**	**6**	**1.0**	**1**	**0.5**	**1**	**0.4**		
Equisetum sp.	2								1			
Sphagnum sp.	1		2		1							
Lycopodium sp.	1											
Monoletes-type	3		1		4		1					
Botrychium sp.					1							

by Tricolpopollenites (50.8%) and Asteraceae (16.9%). Pollen of *Ephedra* sp., Poaceae, and WAP are absent. Other NAP taxa are Cichoriaceae, Lamiaceae, Rosaceae, Brassicaceae, Ranunculaceae, and Polygonaceae. NPPs are represented by many fruit bodies of *Glomus* sp. fungi, and hyphae and spores of unidentified fungal taxa.

PC3 is associated with the loess-like loam, with rare mammal remains of the upper bone-bearing level, and the middle part of the Holocene soil horizon. Pollen of *Betula* sp. dominates in the AP group of all samples. However, changes in the percentages of other taxa made it possible to divide PC3 into two subcomplexes: PC3a and PC3b (Table 5; Fig. 14). Also in all samples, NPPs contain fruit bodies of *Glomus* sp. fungi, and hyphae and spores of unidentified fungal taxa, and phytoliths of unidentified dicotyledons and Poaceae, and chitinous remains of invertebrates.

PC3a (PSs of samples 13, 14) contains an AP 4.8–5.9% of the main percentage sum. In addition to *Betula* sp., pollen of *Pinus* spp. is present sporadically. The NAP (94.1–95.2%) mainly consists of Tricolpopollenites and Asteraceae. Pollen of *Ephedra* sp. and Poaceae are constantly present. The content of *Artemisia* sp. increases from 9.6 to 21.1%, and decreases from 2.9% to a single grain of Chenopodiaceae. WAP is represented by single grain of Cyperaceae gen. indet. Rare spores belong to *Lycopodium* sp. and ferns with Monoletes-type spores.

PC3b (PS of sample 15) shows the amounts of AP and NAP as 3.7% and 96.3%, respectively. The taxonomic composition of pollen did not change compared to PC3a, but *Betula* sp. decreased, and the amount of *Artemisia* sp. increased. The WAP is represented by a single grain of Cyperaceae gen. indet. For the first

Table 4. Number and share of pollen grains and spores in samples 7–12 (AP and NAP as % of the main percentage sum, WAP and spores as % of AP+NAP).

Taxonomic composition	7	%	8	%	9	%	10	%	11	%	12	%
AP	**17**	**6.7**	**19**	**6.5**	**36**	**19.4**	**21**	**7.5**	**18**	**6.3**	**12**	**4.7**
Picea sp.	2	0.8			1	0.5						
Pinaceae gen. indet.	3	1.2	11	3.7	9	4.8	6	2.2	7	2.5	7	2.8
Pinus s/g Diploxylon	5	2.0	3	1.0	15	8.1	7	2.5	1	0.4		
Pinus s/g Haploxylon	1	0.4			2	1.1	1	0.4	3	1.1		
Betula sp.					8	4.3	1	0.4	4	1.4	5	2.0
Populus sp.			3	1.0			1	0.4	2	0.7		
Salicaceae gen. indet.	6	2.4	2	0.7	1	0.5	5	1.8	1	0.4		
NAP	**237**	**93.3**	**275**	**93.5**	**150**	**80.6**	**258**	**92.5**	**267**	**93.7**	**242**	**95.3**
Ephedra sp.	1	0.4			2	1.1						
Asteraceae gen. indet.	6	2.4	43	14.6	12	6.5	18	6.5	24	8.4	43	16.9
Artemisia sp.	34	13.4	14	4.8	12	6.5	15	5.4	19	6.7	12	4.7
Chenopodiaceae gen. indet.	6	2.4	1	0.3	7	3.8	20	7.2	34	11.9	16	6.3
Poaceae gen. indet.	5	2.0			2	1.1	2	0.7	8	2.8		
Tricolpopollenites	84	33.1	123	41.8	78	41.9	112	40.1	114	40.0	130	51.2
Other	101	39.8	94	32.0	37	19.9	91	32.6	68	23.9	41	16.1
Total (AP+NAP)	**254**	**100**	**294**	**100**	**186**	**100**	**279**	**100**	**285**	**100**	**254**	**100**
WAP	**10**	**3.9**	**6**	**2.2**	**13**	**7.0**	**6**	**2.2**	**4**	**1.6**		
Cyperaceae gen. indet.	5		2		4		4		3			
Potamogeton sp.	5		4		9		2		1			
Spores	**1**	**0.4**	**1**	**0.3**					**1**	**0.4**	**3**	**1.2**
Lycopodium sp.											1	
Monoletes-type	1		1						1		2	

time, a significant number of spores (5.4% of AP + NAP), mainly of *Sphagnum* sp., is detected.

The recent PC, although heterogeneous in the content of taxa, is generally of a harmonious type (Table 5, Fig. 14). In PSs of samples A, B and C, the AP content is in the range of 35.8–55.1% of the main percentage sum. In samples A and C, pollen of *Pinus* spp. predominates; and in sample B, *Betula* sp. is the main taxon. Besides, pollen of *Picea* sp. and *Abies* sp. is identified. The amount of NAP is 44.9–64.2% of the main percentage sum. Chenopodiaceae dominates in this group; Poaceae (including cultivated cereals), Tricolpopollenites, Asteraceae, and *Artemisia* sp. are constantly present. *Ephedra* sp. is found in the PS of sample C. Other NAP includes Caryophillaceae, Scrophulariaceae, Rosaceae, Brassicaceae, Ranunculaceae, Rubiaceae, Polygonaceae, and cultivated plants (Boraginaceae, Malvaceae, and Liliaceae). The WAP is represented by Cyperaceae gen. indet., *Potamogeton* sp., *Sparganium* sp., and Numphaeaceae. Spores belong to *Sphagnum* sp., *Equisetum* sp., and ferns with Monoletes-type spores.

AP content in the PS of sample D is 81.9% of the main percentage sum. The dominant taxa are *Pinus* spp. and *Salix* sp. The NAP is represented by *Ephedra* sp., Tricolpopollenites, Asteraceae, and *Artemisia* sp.; other NAP includes Brassicaceae, Lamiaceae, Malvaceae, Onagraceae, Ranunculaceae, Rosaceae, Silenaceae, and Rubiaceae. The WAP (dominated by Cyperaceae) accounts for 40.7% of AP + NAP. The amount of spores, mainly *Equisetum* sp., is 46.7% of AP + NAP.

NPPs in all recent samples are very diverse and present in large numbers. The fruit bodies of *Glomus* sp. fungi, hyphae and various spores of fungal taxa, and phytoliths were noted. In addition, the remains of amoeba and algae, including *Pediastrum* sp., were identified.

Paleoenvironmental stages

After summarizing the results of the geological and palynological data, the following interpretation can be proposed. Four stages of environmental development are revealed for the eastern part of the Baraba Lowland from ca. 20 ^{14}C ka BP to the present.

The first stage (PC1) probably lasted over one thousand years (the lower limit has not yet been determined) and ended ca. 20 ^{14}C ka BP. It reflects a sharp decrease in the level of a large lake-like water body, and the beginning of active erosion of drained coastal areas. Newly formed open spaces were occupied by forb-mesophytic meadows. This caused a sharp increase of the herb pollen content in PC1b against a background of unchanged taxonomic composition of trees. Taiga-type forests occupied the rest of the territory. Among the trees, pines dominated, but birch, spruce, and fir were also present. Despite shallowing, the water reservoir surrounding VG played a significant role.

Table 5. Number and share of pollen grains and spores in samples 13–15, A–D (AP and NAP as % of the main percentage sum, WAP and spores as % of AP+NAP).

Taxonomic composition	13	%	14	%	15	%	A	%	B	%	C	%	D	%
AP	**10**	**4.8**	**14**	**5.9**	**9**	**3.7**	**175**	**35.8**	**213**	**52.2**	**141**	**55.1**	**272**	**81.9**
Abies sp.									1	0.2	19	7.4	1	0.3
Picea sp.									1	0.2	6	2.4	1	0.3
Pinaceae gen. indet.	1	0.5					3	0.6	4	1.0			4	1.2
Pinus s/g Diploxylon	1	0.5	1	0.4	1	0.4	93	19.0	48	11.8	24	9.4	222	66.9
Pinus s/g Haploxylon							9	1.8	4	1.0	49	19.1	22	6.6
Betula sp.	8	3.8	13	5.5	8	3.3	69	14.1	153	37.5	43	16.8	21	6.3
Populus sp.							1	0.2						
Salicaceae gen. indet.									2	0.5			1	0.3
NAP	**199**	**95.2**	**223**	**94.1**	**232**	**96.3**	**314**	**64.2**	**195**	**47.8**	**115**	**44.9**	**60**	**18.1**
Ephedra sp.	2	1.0	1	0.4	1	0.4							1	0.3
Asteraceae gen. indet.	24	11.5	35	14.8	24	10.0	5	1.0	4	1.0	5	2.0	4	1.2
Artemisia sp.	20	9.6	50	21.1	61	25.3	26	5.3	8	2.0	5	2.0	8	2.4
Chenopodiaceae gen. indet.	6	2.9	1	0.4	1	0.4	178	36.4	116	28.4	77	30.1	17	5.1
Poaceae gen. indet.	5	2.4	6	2.5	6	2.5	23	4.7	20	4.9	5	2.0	15	4.5
Tricolpopollenites	96	45.9	97	40.9	82	34.0	9	1.8	3	0.7	1	0.4	3	0.9
Other	46	22.0	33	13.9	57	23.7	73	14.9	44	10.8	22	8.6	12	3.6
Total (AP+NAP)	**209**	**100**	**237**	**100**	**241**	**100**	**489**	**100**	**408**	**100**	**256**	**100**	**332**	**100**
WAP	**1**	**0.5**			**1**	**0.4**	**7**	**1.4**	**5**	**1.2**	**6**	**2.3**	**138**	**41.6**
Cyperaceae gen. indet.	1				1		6		4		6		135	
Potamogeton sp.													3	
Sparganium sp.							1							
Numphaeaceae gen. indet.									1					
Spores	**4**	**1.9**	**1**	**0.4**	**13**	**5.4**	**11**	**2.2**	**13**	**3.2**	**23**	**9.0**	**155**	**46.7**
Equisetum sp.							1		1		10		150	
Sphagnum sp.					10		6		10		9		4	
Lycopodium sp.	1												1	
Monoletes-type	3		1		3		4		2		4			

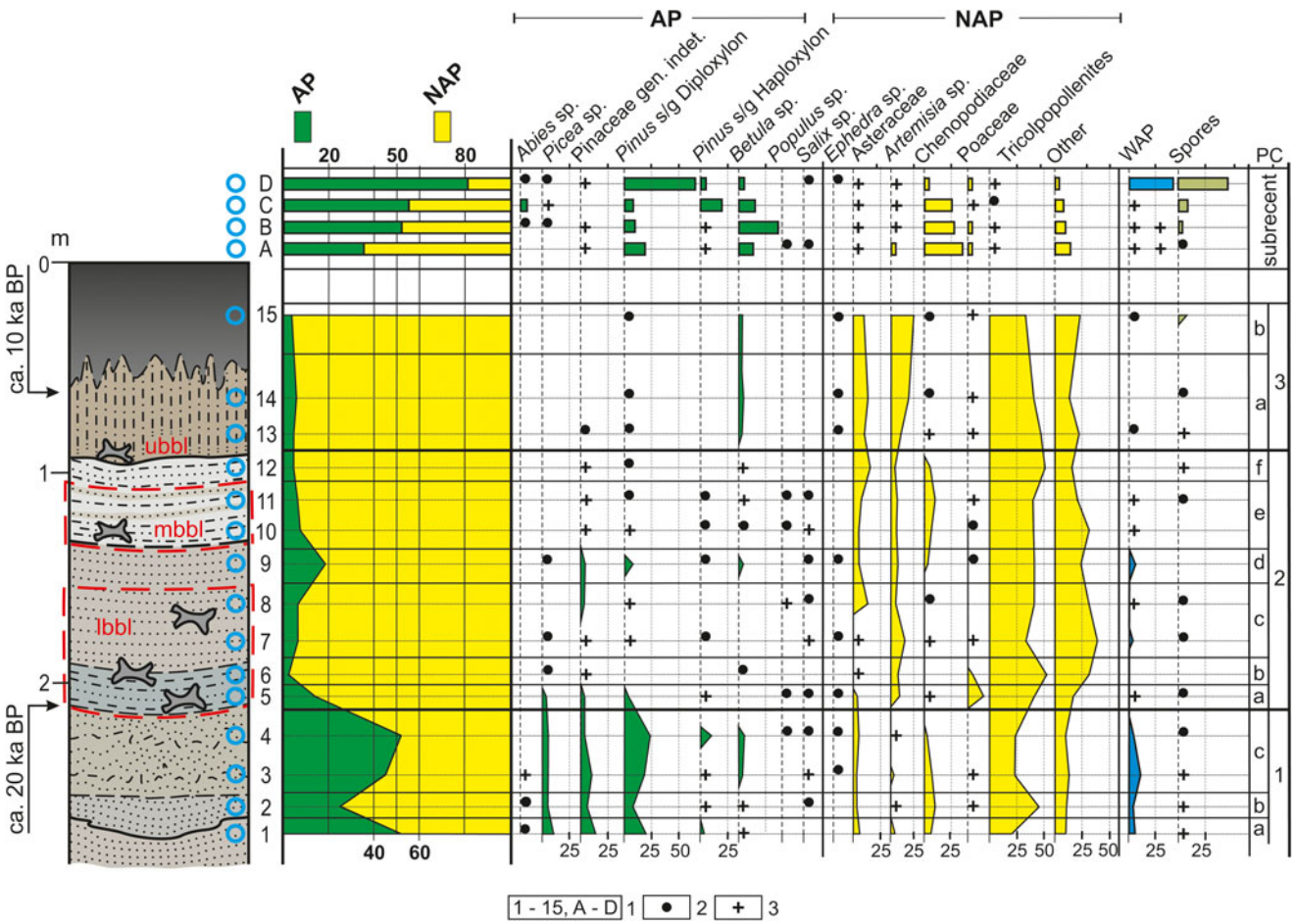

Figure 14. Pollen diagram for sediments of the VG central faunal assemblage (2016 excavations). 1 = sample numbers; 2 = very rare pollen grains and spores; 3 = content up to 3% (AP and NAP of the main percentage sum, WAP and spores of AP+NAP; abbreviations in the Table 3). Other symbols in Figure 7.

Willows and sedges grew in its coastal part, and cattail and pondweed grew in shallow waters.

The second stage (PC2) began ca. 20 ^{14}C ka BP and lasted no less than 6000–8000 years. This is the main formation period of the bone-bearing horizon. At that time, the climate became arid and led to a sharp degradation of forests. Forb-grass steppe became widespread. Saline lands and alkali meadows developed within the region, as indicated by the pollen of Plumbaginaceae (Limonium-type). Nevertheless, the lake continued to exist in the immediate vicinity of VG, although its level was not stable. During the period of accumulation of sediments separating the lower and middle bone-bearing levels, there was an increase in the proportion of trees with a dominance of pines (PC2d). At the same time, lake level increased, which led to the flooding of coastal areas and expansion of coastal and aquatic vegetation. There was a significant degradation of the lake in the final phase of this stage (PC2f).

The third stage (PC3) began at the end of the late glacial period, and ceased probably in the second half of the Holocene. Aridity of the climate increased. Loess-like loam containing rare mammal remains of the upper bone-bearing level was formed under conditions similar to those of the modern southern steppes of the West Siberian Plain, as indicated by the composition of rare tree pollen with a complete dominance of birch (PC3a). There were probably no lakes in the surrounding area. Formation of the Holocene soil horizon began after a hiatus. However low area bogs are recorded for its middle part (PC3b), although the steppes continued to dominate.

The latest stage (PSs A–D) is characterized by the prevalence of forest-steppe. The recent PC adequately reflects the modern regional and local vegetation. The APs of samples A, B, and C do not exceed 55.1% of the main percentage sum, and NAP is presented by a large number of taxa. Such PSs correspond to the forest-steppe zone. The PS of sample D shows an increased amount of AP due to local wetland conditions and excluding WAP from the main percentage sum. In the nearest forest belts, many pines (*Pinus sylvestris* L.) were planted in the twentieth century, and in Mamontovoe Village, spruce (*Picea obovata* Ledeb.) and fir (*Abies sibirica* Ledeb.) were also planted. These trees today are already mature and produce large amounts of pollen. Thus, a significant amount of AP belonging to Pinaceae can be seen in all recent PSs; only in the PS of sample B, which was taken near the birch forest outlier, was pollen of *Betula* sp. a dominant taxon.

DISCUSSION

Analysis of the VG sections and the site's taphonomy indicates that thousands of animal remains were buried here, mainly in mud pits and linear erosion forms. The structure of layers, the crushed bones and their steep-angled position indicate mixture of the sediments and trampling of subfossil skeletons by living

mammoths and other large mammals. We interpret the presence of lithic artifacts as an indication that Paleolithic humans also participated in this process. It is important to note that the conclusion about the burial of mammoth remains in a gully already was made based on results of the initial fieldwork at VG (Polunin, 1961). The first large-scale excavations found evidence of inclined and vertical positions of some bones, and this clearly suggested the existence of mud pits and the presence of trampling. However, these were interpreted by archaeologists as the activity of ancient humans (Okladnikov et al., 1971).

Despite the moistening (likely by sporadic flooding) of local areas within VG, dry environmental conditions prevailed during the formation of this site. Evidence of this is not only the result of palynological analysis, but also irregular open cracks inside the bone-bearing horizon and at the border with the underlying lacustrine-like sediments (Fig. 7). They are diagnosed as desiccation cracks, usually with a width up to several centimeters, although cracks up to 10 cm wide and 0.8 m long were recorded in the 1991 excavation pit (Maschenko and Leshchinskiy, 2001). These dimensions are not the largest ones—similar cracks up to 12.5 cm wide are described in contemporary silty sediments and giant desiccation cracks >3 m long in Mesozoic clay shale (Shrock, 1948; Reineck and Singh, 1975).

Therefore, the upper part of the VG section demonstrates a sharp change from subaqueous to subaerial sedimentation conditions, which is emphasized by the strong carbonatization of sediments at the contact of layers of different genesis, including desiccation cracks (Fig. 7). This points to a high concentration of alkaline earth and alkali elements in the ground and pore waters of sediments that form the geochemical landscape of VG. These elements—primarily Ca, Mg, and Na—and some trace elements create the basis for favorable geochemical landscapes, which are very attractive to large herbivores of past and present times, in particular, representatives of the Proboscidea (Cooper, 1831; Leshchinskiy, 2001, 2012, 2015; Walker et al., 2001; Holdø et al., 2002; Mwangi et al., 2004; Haynes, 2012). At the end of the Pleistocene, mineral starvation caused by chronic geochemical stress led to the concentration of large mammals around the beast solonetz. Here, in addition to vegetation, animals could consume sediments, along with surface and/or groundwater, rich in vital macro- and microelements (Leshchinskiy, 2006, 2009, 2015). Thus, lithophagy was probably the main reason for the visits of megafauna to the VG.

The abnormal diet of VG mammals is confirmed by the isotopic composition of bone collagen (Table 2; Figs. 12, 13). The available nutritional data on the late Pleistocene populations of Europe, Siberia, and Eastern Beringia indicate their sharp difference from those at the VG site (Figs. 15, 16). This is clear from the $\delta^{15}N$ value, which for most VG mammoths is between 13.00‰ and 15.00‰, with only one individual having a significantly lower $\delta^{15}N$ value (7.90‰). For comparison, these ratios in late Pleistocene mammoths are not greater than 12.60‰, and their average values for the interval 20–10 ^{14}C ka BP are <10‰. The $\delta^{15}N$ ratios of the VG fox and wolves varied from 16.20–17.10‰, which significantly exceeds values for these carnivores during the late Pleistocene and Holocene (3.90–14.20‰). The $\delta^{13}C$ values of the VG mammoths are in the middle of the range for this species, and the VG fox and wolf $\delta^{13}C$ values are from −18.82‰ to −16.89‰, which are possibly the maximum for canids of Europe, Siberia, and Eastern Beringia (Bocherens et al., 1996; Bocherens and Drucker, 2003; Szpak et al., 2010; Drucker et al., 2015, 2017, 2018; Jürgensen et al., 2017;

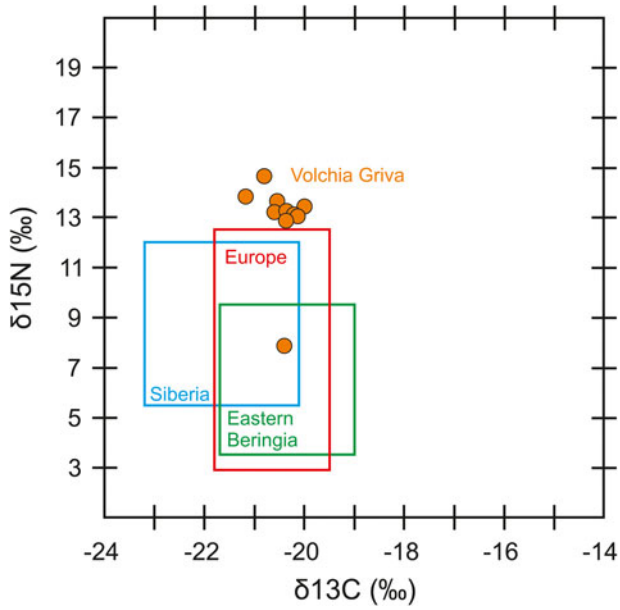

Figure 15. The $\delta^{13}C$ and $\delta^{15}N$ values of woolly mammoth bone collagen from VG (circles), compared to ranges from Europe (red box), Siberia (blue box), and Eastern Beringia (green box) (Bocherens et al., 1996; Szpak et al., 2010; Drucker et al., 2015, 2018; Seuru et al., 2017; Kuitems et al., 2019; Kuzmin et al., 2021).

Rabanus-Wallace et al., 2017; Seuru et al., 2017; Kuitems et al., 2019; Wißing et al., 2019; Kuzmin et al., 2021). The single isotopic values of the VG horse and bison bones can be considered as preliminary.

The results of isotopic studies demonstrate the special nutritional characteristics of the VG mammoth fauna. The very high mammoth $\delta^{15}N$ values are noteworthy, and are expected for the ecosystem of the fertile forb-grass mammoth steppe under

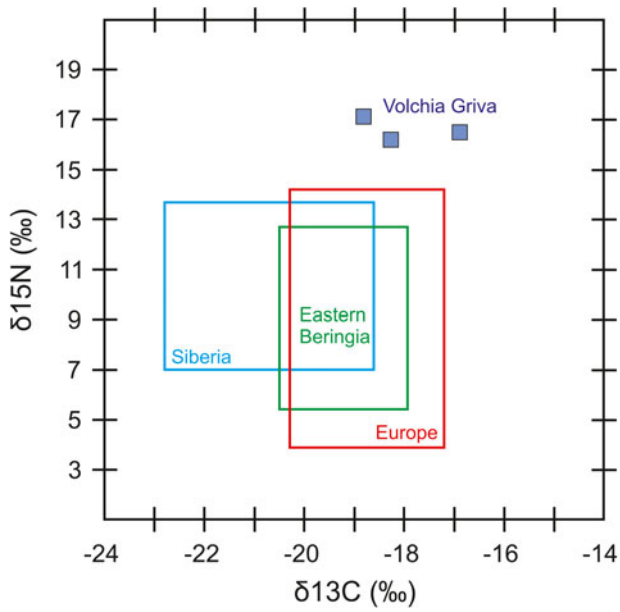

Figure 16. The $\delta^{13}C$ and $\delta^{15}N$ values of canine bone collagen from VG (squares), compared to ranges from Europe (red box), Siberia (blue box), and Eastern Beringia (green box) (Bocherens et al., 1996; Bocherens and Drucker, 2003; Bocherens, 2015; Drucker et al., 2017, 2018; Kuzmin et al., 2021).

conditions of favorable geochemical landscapes. Moreover, VG mammoths showed higher $\delta^{15}N$ values than both horse and bison, and these are consistent with the canine $\delta^{15}N$ values, which were observed previously in studies of the late Pleistocene mammoth steppe and suggested by the classic isotopic model (Bocherens et al., 1996; Fox-Dobbs et al., 2008; Bocherens, 2015; Drucker et al., 2018). At VG, the canine $\delta^{13}C$ and $\delta^{15}N$ values are higher than those of mammoth, horse, and bison, which are consistent with trophic enrichment of the carnivores. The fox and wolves analyzed at VG showed similarly high $\delta^{13}C$ and $\delta^{15}N$ values, which could indicate that large herbivores were the basis of their diet (in which case, the foxes were scavengers). The differences between the $\delta^{13}C$ and $\delta^{15}N$ values in the bone collagen of VG canids, on the one hand, and the coeval mammoth and horse from VG, on the other hand, are ~2.1 ± 1.8‰ and ~3.2 ± 1.6‰. This is similar to the estimates for $\delta^{13}C$ and the $\delta^{15}N$ differences between the collagen of predators and their average prey, obtained from modern and archaeological data: 1.1 ± 0.2‰ and 3.8 ± 1.1‰, respectively (Bocherens, 2015). At the same time, the relatively low $\delta^{15}N$ values of a bison and one mammoth most likely indicate long-term migrations of several large mammal populations from remote areas where environmental conditions were worse than at VG.

In any case, at the peak of mineral deficiency, dozens (possibly hundreds, especially during migrations, rutting, lactation, etc.) of large mammals were concentrated at VG. Their relatively high mortality and favorable conditions for burial of their remains contributed to the formation of the discontinuous, but still very rich, bone-bearing horizon. The taphonomic differences and changes in the geological structure of the VG site along its expanse are important. As noted above, the bone-bearing horizon in the northeastern assemblage is a single body (Figs. 2, 3). Slow subaerial sedimentation was the reason for the superimposition of faunal remains of different ages. Therefore, the allocation of three levels in the northeastern part of VG is arbitrary, and is associated with the excavation technique used (Maschenko and Leshchinskiy, 2001; Leshchinskiy et al., 2008, 2015). The faunal remains were buried in a semi-flat, low depression, which turned into a mud pit when conditions became wet. However, despite the obvious trampling of individual bones, the zero stage of bone weathering here is absent or very rare. This indicates a long exposure of animal carcasses on the ground surface: for the upper and middle parts of the bone-bearing horizon, where stages 4 and 5 prevail, it can be estimated as >10–25 years, and for the bottom of the bone-bearing stratum, where weathering is mainly of stages 2 and 3, at least five years after the death of animals (Behrensmeyer, 1978; Haynes, 1999).

The bone-bearing horizon of the central assemblage sometimes can be divided into three levels (Figs. 4–9). In the lower level, the remains are perfectly preserved. They have mainly weathering stages 0 and 1, which is associated with rapid burial in a local erosional form (small gully), probably up to three years after the death of animals. The overlying remains from the middle level were confined to those already present in the lower level, which from time to time turned into a typical mud pit. Therefore, the taphonomic characteristics of the middle and upper levels, where animal remains are very rare (possibly, re-deposited), are almost the same here as in the northeastern assemblage.

Modern elephants often move the bones and tusks of deceased relatives, especially in places of their concentration (e.g., near watering sites and on mineral licks). They also transform the microrelief by digging large pits and even caves using tusks and limbs during their search for mineral-containing sediments (Haynes, 2012). This behavior probably also was typical for mammoths, which could greatly alter the primary structure of thanatocoenosis and stratigraphy at faunal localities. Therefore, inversions of ^{14}C dates recorded at VG and other large megafaunal sites (Table 2; Derevianko et al., 2000; Leshchinskiy et al., 2008) are not always the result of errors associated with poor sampling, contamination, or other flaws of either researchers or the ^{14}C dating method. Such inversions can be explained by the re-deposition of bones, trampling, digging, and other taphonomic phenomena, including human activity.

Nevertheless, the new results of radiocarbon dating show a sharp peak of mammoth mortality at the VG during the period of ca. 20–18 ^{14}C ka BP, and a smoothed peak at ca. 17–11 ^{14}C ka BP (Tables 1, 2). This largely corresponds to the lower and middle bone-bearing levels, the formation of which indicates high levels of animal activity on the beast solonetz. If lithophagy was the main reason for animals to visit VG, it reflects two waves of geochemical stress of the mammoth fauna. At the same time, the oldest ^{14}C dates were obtained on horse bones, although they did not occupy the lowest position in the sections. Perhaps, this is a case related to an insufficient degree of sampling. Another explanation may be that the horses were more mobile than mammoths, which allowed them to be the first to occupy drained spaces with favorable geochemical landscapes.

The 2015–2018 research showed that the mammoths of the Baraba refugium at the LGM were significantly larger compared to mammoths of the late glacial period. The presence of very large and small adult individuals and two morphological types of teeth in the bone-bearing horizon of VG was already noted when material from the northeastern assemblage of 1991 was examined (Maschenko and Leshchinskiy, 2001). Today this fact can be explained by the superimposition of faunal remains of different ages that belong to two different mammoth populations, separated in time by at least 1000 years. This is not an anomaly, but reflects the general trend of adaptive size reduction when mammoth mortality at the end of the Pleistocene was high (Leshchinskiy, 2006, 2015).

The large local concentration of mammoth remains at VG (50 to >130/m^2 in the 2015–2018 excavations area) can be compared with the alluvial site of Berelyokh (Northern Yakutia), where in some sectors specimens numbering up to 50/m^3 were recorded (Vereshchagin, 1977). Thus, today the VG mammoth concentration is the highest in Asia with in situ burial conditions. Obviously, the initial concentration of remains at the VG subaerial thanatocoenosis was even higher, since significant weathering and carnivores completely destroyed a certain number of bones, especially of calves. Despite this, preliminary results of new investigations confirm the conclusion of a high proportion of immature mammoths in the age profiles of MIS 2 (Sartanian according to the Western Siberia stratigraphic scale) sites in Siberia (Leshchinskiy, 2015, 2017). It should be noted that the identified minor role of predators and scavengers in the formation of the VG site may be an underestimate, since the outer lamellar compact bone, on which small traces of tooth marks can be observed, is usually absent at weathering stages 3–5. This is also true for the thin cut marks on bones made by ancient humans.

Humans actively hunted large mammals, and they most probably also killed mammoths, but relatively rarely—for example, when mammoths fell into natural traps or were weak (pregnant females, or injured, sick, exhausted, and old individuals, or

young animals) (Zenin et al., 2006). At VG, people also could have used the remains of mammoths that died because of predators, diseases, injuries, and other causes. Moreover, human visits to VG were purposeful and systematic in nature because most of the artifacts found here are 'exotic'—made of rock crystal and smoky quartz, the sources of which are located several hundred kilometers from VG (Leshchinskiy et al., 2021b). Similar conclusions were made after studying other large subaerial and lacustrine-alluvial mammoth sites of the late Pleistocene in Siberia (Vereshchagin, 1977; Derevianko et al., 2000; Zenin et al., 2006; Seuru et al., 2017).

The taxonomic composition of mammals and the results of analysis of geological sections and taphonomy at VG are fully consistent with the data provided by palynological studies. Representative materials of pollen, spores, and other microfossils, together with the data presented above, for the first time made it possible to reconstruct in detail the history of landscape changes in the Baraba Lowland during the Sartanian in Siberia.

The natural environment before accumulation of the bone-bearing horizon was quite different from the contemporary one (e.g., conditions were wetter than today). This was determined by palynological data, using the presence of forest areas of the taiga-type, with a significant role of spruce. However, since the beginning of the formation of the megafaunal site, a pronounced aridization of the climate occurred. The open spaces of the mammoth steppe were widespread, where forb-grass associations with areas of alkaline meadows and alkali soils dominated.

Thus, at ca. 20 ^{14}C ka BP, the forests in the Baraba Lowland disappeared. Since this time, steppes dominated at least until the mid-Holocene. It is important to note that in the middle part of the Holocene soil horizon, for the first time a relatively large amount of *Sphagnum* sp. spores are recorded, and this indicates the development of swamps. This is consistent with data on the beginning of paludification of the lakes in the south of the West Siberian Plain since ca. 6–5.5 ^{14}C ka BP (Orlova, 1990; Levina and Orlova, 1993; Liss et al., 2001; Krivonogov et al., 2018). The domination of open landscapes with rich herb cover from the last glacial maximum to the mid-Holocene is confirmed by the remains of woolly mammoth, horse, bison, and other representatives of the megafauna found in the Baraba Lowland where, in addition to VG, such finds were made at other sites (van der Plicht et al., 2015; Puzachenko et al., 2017).

Currently, the Baraba Lowland is located in the forest-steppe zone of the Ob-Irtysh interfluve. Open landscapes, unchanged by human activities, are covered with steppe halophytic-grass meadows. In forest outliers, birch dominates; willow and aspen are also found. The modern climate is markedly continental. According to observations from the middle of the twentieth century, the average air temperatures are (at the nearest meteorological stations in Kamen-on-Ob and Barabinsk): for July 18.3–19.7°C, and for January −19.1–18.2°C. The average annual temperature is 0.5–1.2°C, with a range of 85– 95°C. The annual precipitation is 315–450 mm (Arhiv klimaticheskih dannyh, 2012; Pogoda i klimat, 2020).

Several scenarios for development of the natural environment during the Sartanian were previously proposed for the Baraba Lowland. They were mainly based on geological and geomorphological data, and the studies of paleosols and mammoth fauna. The lack of associated palynological data was a serious obstacle to the in-depth analysis of past natural conditions. The nearest sections, in which pollen and spore complexes of the MIS 2 period were identified, are located in the steppe and taiga zones, 250–440 km south and north of VG. Therefore, reconstructions obtained by extrapolating the results of palynological and biome analyses from neighboring territories are basically hypothetical (Arkhipov and Volkova, 1994; Tarasov, 2000; Binney et al., 2017). However, some of them also suggested the prevalence of cold forb-grass and wormwood-forb steppes in this region (Grichuk, 2002).

In general, the terminal Pleistocene in the south of the West Siberian Plain was characterized by extreme environmental conditions. Some authors attributed this to the existence of the giant ice-dammed Lake Mansi, whose bays penetrated far into the Baraba Lowland (Arkhipov and Volkova, 1994; Volkova and Mikhailova, 2001). Therefore, this area on the paleogeographic maps for the last glacial maximum is often represented by forest-tundra and green-moss bogs. According to the same data for the late glacial period, a transformation into dry tundra probably occurred, in which xerophyte-Chenopodiaceae associations dominated. It was assumed that the average annual air temperature at that time dropped to −11°C. Other authors suggested that the entire West Siberian Plain during ca. 20–11 ^{14}C ka BP was a region of maximum aridization (i.e., a cold desert); in the south, loess accumulation predominated (Velichko et al., 2011). This concept is shared by researchers working in the Lake Aksor depression (51°27′N, 77°47′E) in the extreme south of the West Siberian Plain. For the first half of the Sartanian, a desert regime with wind erosion was prevalent here; during periodic wettings, a lake was formed and drained eight times, and afterwards it drained. Moreover, the authors note an extreme range of average annual temperatures between −3°C and −20°C (Zykin et al., 2002; Zykin and Zykina, 2009). Notably, supporters of both concepts mentioned above consider aeolian activity as the main agent for the formation of elongated mounds in the Baraba Lowland. Altogether, this implies very severe environmental conditions, which supposedly made vast territories poorly suitable for existence of large mammals.

The traditional environmental reconstructions presented above are not confirmed by the latest studies of VG, which indicate widespread occurrence of forb steppe landscapes from ca. 20 ^{14}C ka BP to the mid-Holocene. The concepts of Lake Mansi and the cold desert come into apparent conflict with the geological structure of the Baraba Lowland. Our research indicates water erosion origins of elongated mounds, which are only covered with thin subaerial sediments that rarely exceed a thickness of 1.5 m. A similar conclusion was put forward at the beginning of the twentieth century, and the hypothesis of Eurasian hydrosphere catastrophes was formed, explaining the mechanism of formation of the elongated mound relief (Petrov, 1948; Grosswald, 1999). Despite a number of problematic issues, this hypothesis has been actively put forward in recent years (e.g., Komatsu et al., 2016). Modern data indicate the absence of continental glaciation in Western Siberia and the presence of free north-flowing rivers in MIS 2 (Mangerud et al., 2004). Therefore, a new discussion arose about a large lake-like water body in the Baraba Lowland at the beginning of MIS 2 and its sharp reduction with non-cyclic fluctuations in water level after ca. 20 ^{14}C ka BP. Our geological and palynological data (Fig. 14) clearly favor this scenario. Perhaps this reservoir was associated with surface water flows, which, according to some authors, could have arisen during catastrophic flood events caused by outbursts of the glacier-dammed lakes in the Altai Mountains (Agatova et al., 2020; Herget et al., 2020). However, more research is needed to confirm or refute this hypothesis.

CONCLUSIONS

The unique combination of depressions of the VG microrelief with the periodic death of animals within it explains the formation of a mammoth fauna site at this locus. The favorable geochemical landscape of the beast solonetz for a long period (ca. 20–10 ^{14}C ka BP) attracted large Pleistocene animals, the remains of which formed an extensive and thick bone-bearing horizon. Within the last glacial maximum and late glacial, two peaks of high mortality for large mammals were established, and they generally may reflect waves of geochemical stress on animal populations. Humans were both witnesses to and participants in this process. However, the rarity of lithic artifacts and the absence of direct evidence of mammoth hunting and butchering of their carcasses confirm that the VG site was primarily a place of natural death for the megafauna.

The high mortality of large herbivores in a limited area is explained by periodic visits of animals to the mineral oasis for millennia. In certain seasons, the concentration of animals could have reached several hundred, and some weak individuals would have been easy prey for carnivores, died from exhaustion, diseases, or a combination of different factors. Bones with various signs of osteodystrophy convincingly indicate that this is a likely scenario. Thus, the presence of thousands of mammoth remains at VG probably shows chronic mineral starvation during the last mass extinction.

The large area and a record concentration of faunal remains put the VG site into the category of the largest in situ mammoth fauna locality in Asia. At present, no more than 5% of the site's total area, which may amount to several hectares, has been excavated. Most likely, in the well known central assemblage alone, >10,000 bones and teeth of mammoths, as well as other late Pleistocene mammals, were buried. The long formation period, unique taphonomic conditions, relatively high concentration of pollen and spores in sediments, and the availability of human-related materials (artifacts) testify in favor of the highest prospects for interdisciplinary research in the coming decades.

It should be emphasized that the presented environmental reconstruction is currently the most complete for the Baraba Lowland at ca. 20–10 ^{14}C ka BP (PC1–PC3a). For the first time, it reliably shows the wide distribution of steppes in the south of the West Siberian Plain in that period. Thus, the VG site as a whole is now one of the main objects to investigate the late Pleistocene ecosystems of Northern Eurasia.

Acknowledgments. We are deeply indebted to A.V. Gulina, N.Ya. Fedyaev, A.T. Dzhumanov, A.S. Samandrosova, A.S. Semiryakov, E.V. Kanishcheva, S.S. Perfilev, N.A. Shilovskiy, E.Yu. Samoylova, D.V. Tumantseva, A.Yu. Kolesova, and A.A. Zolotarev (TSU); V.N. Zenin and A.A. Dudko (Institute of Archaeology and Ethnography, Siberian Branch of the Russian Academy of Sciences, Novosibirsk, Russia); S.A. Kravchuk and N.S. Kravchuk (Berdsk Town, Russia); D.Y. Kadochnikov (Mamontovoe Village, Russia); U. Ratajczak and A. Kotowski (University of Wrocław, Poland); and Ya.S. Trubin and N.V. Utkin (Industrial University of Tyumen, Russia) for the comprehensive assistance in conducting field and laboratory studies. Many thanks to B.N. Ermakov and S.V. Gayduk, heads of the local administration in 2015–2016 and 2017–2018, for support and the opportunity to conduct excavations within Mamontovoe Village. We also are grateful to S.G. Keates and Y.V. Kuzmin for polishing the English.

Expeditions were conducted within the TSU Competitiveness Improvement Program, and the State Task of the Ministry of Education and Science of the Russian Federation, Project No. 5.4217.2017/4.6. The main laboratory research, final processing of the paleontological materials, and comparative analysis were funded by the Russian Science Foundation, Grant No. 20-17-00033.

REFERENCES

Agatova, A.R., Nepop, R.K., Carling, P.A., Bohorquez, P., Khazin, L.B., Zhdanova, A.N., Moska, P., 2020. Last ice-dammed lake in the Kuray basin, Russian Altai: new results from multidisciplinary research. *Earth-Science Reviews* **205**, 103183. https://doi.org/10.1016/j.earscirev.2020.103183.

Alexeeva, E.V., Vereshchagin, N.K., 1970. Mammoth hunters in the Baraba steppe. *Priroda* **1**, 71–74. [in Russian]

Ambrose, S.H., 1990. Preparation and characterization of bone and tooth collagen for isotopic analysis. *Journal of Archaeological Science* **17**, 431–451.

Arhiv klimaticheskih dannyh, 2012. http://climatebase.ru/ (accessed 10 June 2020).

Arkhipov, S.A., Volkova, V.S., 1994. *Geological History, Pleistocene Landscapes and Climate in West Siberia*. NIC OIGGM SO RAN, Novosibirsk. [in Russian]

Babin, G.A., Chernykh, A.I., Golovina, A.G., Zhigalov, S.V., Dolgushin, S.S., Vetrov, E.V., Korableva T.V., *et al.*, 2015. *Gosudarstvennaya geologicheskaya karta Rossiyskoy Federacii. Masshtab 1:1000000 (tretye pookoleniye). Seriya Altaye-Sayanskaya. List N-44–Novosibirsk*. Kartograficheskaya fabrika VSEGEI, St. Petersburg. [in Russian]

Baryshnikov, G.F., Kuzmina I.T., Hrabrii V.M., 1977. Rezultaty izmerenii trubchatyh kostey mamontov Berelyokhskogo "kladbishcha". In: Starobogatov, Ja.I. (Ed.), *Mamontovaya fauna Russkoy ravniny i Vostochnoy Sibiri*. Proceedings of the Zoological Institute 72, Academy of Sciences of the USSR, Leningrad, pp. 58–67. [in Russian]

Behrensmeyer, A.K., 1978. Taphonomic and ecologic information from bone weathering. *Paleobiology* **4**, 150–162.

Binney, H., Edwards, M., Macias-Fauria, M., Lozhkin, A., Anderson, P., Kaplan, J.O., Andreev, A., *et al.*, 2017. Vegetation of Eurasia from the last glacial maximum to present: key biogeographic patterns. *Quaternary Science Reviews* **157**, 80–97.

Bocherens, H., 2015. Isotopic tracking of large carnivore palaeoecology in the mammoth steppe. *Quaternary Science Reviews* **117**, 42–71.

Bocherens, H., Drucker, D., 2003. Trophic level isotopic enrichment of carbon and nitrogen in bone collagen: case studies from recent and ancient terrestrial ecosystems. *International Journal of Osteoarchaeology* **13**, 46–53.

Bocherens, H., Pacaud, G., Lazarev, P., Mariotti, A., 1996. Stable isotope abundances (^{13}C, ^{15}N) in collagen and soft tissues from Pleistocene mammals from Yakutia. Implications for the paleobiology of the mammoth steppe. *Palaeogeography, Palaeoclimatology, Palaeoecology* **126**, 31–44.

Braun, I.M., Palombo, M.R., 2012. *Mammuthus primigenius* in the cave and portable art: an overview with a short account on the elephant fossil record in Southern Europe during the last glacial. *Quaternary International* 276–277, 61–76.

Bukreyeva, G.F., Poleshchuk, V.P., 1970. Baraba steppe. In: Saks, V.N. (Ed.), *History of the Evolution of the Vegetation of the Extraglacial Region in Late Pliocene and Quaternary Time*. Transaction of the Institute of Geology and Geophysics 92, Siberian Branch of Academy of Sciences of the USSR, Moscow, pp. 128–164. [in Russian]

Chepurov, K.P., Cherkasova, A.V., Akulov, N.M., Ostrovskiy, I.I., Martynyuk, D.F., 1955. *Urovskaya Bolezn*. Amurskoe knizhnoe izdatelstvo, Blagoveshchensk. [in Russian]

Chlachula, J., Serikov, Yu.B., 2010. Last glacial ecology and geoarchaeology of the Central Trans-Ural area: the Sosva River Upper Palaeolithic Complex, western Siberia. *Boreas* **40**, 146–160.

Christiansen, P. 2004. Body size in proboscideans, with notes on elephant metabolism. *Zoological Journal of the Linnean Society* **140**, 523–549.

Clarke, E.A., Goodship, A.E., 2010. A severely disabled mammoth—the palaeopathological evidence. *Quaternary International* **228**, 210–216.

Cooper, W., 1831. Notices of big-bone lick. *The Monthly American Journal of Geology and Natural Science* **1**, 158–174, 205–217.

Dehasque, M., Pečnerová, P., Muller, H., Tikhonov, A., Nikolskiy, P., Tsigankova, V.I., Danilov, G.K., *et al.*, 2021. Combining Bayesian age models and genetics to investigate population dynamics and extinction of the last mammoths in northern Siberia. *Quaternary Science Reviews* **259**, 106913. https://doi.org/10.1016/j.quascirev.2021.106913.

Derevianko, A.P., Zenin, V.N., Leshchinskiy, S.V., Mashchenko, E.N., 2000. Peculiarities of mammoth accumulation at Shestakovo site in West Siberia. *Archaeology, Ethnology & Anthropology of Eurasia* **3**, 42–55.

Drucker, D., Vercoutère, C., Chiotti, L., Nespoulet, R., Crépin, L., Conard, N.J., Münzel, S.C., *et al.*, 2015. Tracking possible decline of woolly mammoth during the Gravettian in Dordogne (France) and the Ach Valley (Germany) using multi-isotope tracking (^{13}C, ^{14}C, ^{15}N, ^{34}S, ^{18}O). *Quaternary International* 359–360, 304–317.

Drucker, D., Naito, Y.I., Péan, S., Prat, S., Crépin, L., Chikaraishi, Y., Ohkouchi, N., *et al.*, 2017. Isotopic analyses suggest mammoth and plant in the diet of the oldest anatomically modern humans from far southeast Europe. *Scientific Reports* **7**, 6833. https://doi.org/10.1038/s41598-017-07065-3.

Drucker, D.G., Stevens, R.E., Germonpré, M., Sablin, M.V., Péan, S., Bocherens, H., 2018. Collagen stable isotopes provide insights into the end of the mammoth steppe in the central East European plains during the Epigravettian. *Quaternary Research* **90**, 457–469.

El Adli, J.J., Fisher, D.C., Vartanyan, S.L., Tikhonov, A.N., 2017. Final years of life and seasons of death of woolly mammoths from Wrangel Island and mainland Chukotka, Russian Federation. *Quaternary International* **445**, 135–145.

Fisher, D.C., Shirley, E.A., Whalen, C.D., Calamari, Z.T., Rountrey, A.N., Tikhonov, A.N., Buigues, B., Lacombat, F., Grigoriev, S., Lazarev, P.A., 2014. X-ray computed tomography of two mammoth calf mummies. *Journal of Paleontology* **88**, 664–675.

Flueck, W.T., Smith-Flueck, J.A.M., 2008. Age-independent osteopathology in skeletons of a South American cervid, the Patagonian huemul (*Hippocamelus bisulcus*). *Journal of Wildlife Diseases* **44**, 636–648.

Fox-Dobbs, K., Leonard, J.A., Koch, P.L., 2008. Pleistocene megafauna from eastern Beringia: paleoecological and paleoenvironmental interpretations of stable carbon and nitrogen isotope and radiocarbon records. *Palaeogeography, Palaeoclimatology, Palaeoecology* **261**, 30–46.

Grichuk, V.P., 2002. Rastitelnost pozdnego pleistocena. In: Velichko, A.A. (Ed.), *Dinamika Landshaftnyh Komponentov i Vnutrennih Morskih Bassieynov Severnoy Evrazii za Poslednie 130000 let*. GEOS, Moskva, pp. 64–89. [in Russian]

Grosswald, M.G., 1999. *Cataclysmic Megafloods in Eurasia and the Polar Ice Sheets*. Scientific World, Moscow. [in Russian]

Guiry, E.J., Szpak, P., 2021. Improved quality control criteria for stable carbon and nitrogen isotope measurements of ancient bone collagen. *Journal of Archaeological Science* **132**, 105416. https://doi.org/10.1016/j.jas.2021.105416.

Guthrie, R.D., 2004. Radiocarbon evidence of mid-Holocene mammoths stranded on an Alaskan Bering Sea island. *Nature* **429**, 746–749.

Haynes, G., 1991. *Mammoths, Mastodonts, and Elephants: Biology, Behaviour and the Fossil Record*. Cambridge University Press, New York.

Haynes, G., 1999. The role of mammoths in rapid Clovis dispersal. *Deinsea* **6**, 9–38.

Haynes, G. 2012. Elephants (and extinct relatives) as earth-movers and ecosystem engineers. *Geomorphology* 157–158, 99–107.

Haynes, G., Klimowicz, J., 2015. A preliminary review of bone and teeth abnormalities seen in recent *Loxodonta* and extinct *Mammuthus* and *Mammut*, and suggested implications. *Quaternary International* **379**, 135–146.

Herget, J., Agatova, A.R., Carling, P.A., Nepop, R.K., 2020. Altai megafloods—the temporal context. *Earth-Science Reviews* **200**, 102995. https://doi.org/10.1016/j.earscirev.2019.102995.

Holdø, R.M., Dudley, J.P., McDowell, L.R., 2002. Geophagy in the African elephant in relation to availability of dietary sodium. *Journal of Mammalogy* **83**, 652–664.

Johnson, H.E., Bleich, V.C., Krausman, P.R., 2007. Mineral deficiencies in tule elk, Owens Valley, California. *Journal of Wildlife Diseases* **43**, 61–74.

Jürgensen, J., Drucker, D.G., Stuart, A.J., Schneider, M., Buuveibaatar, B., Bocherens, H., 2017. Diet and habitat of the saiga antelope during the late Quaternary using stable carbon and nitrogen isotope ratios. *Quaternary Science Reviews* **160**, 150–161.

Kahlke, R.-D., 1999. *The History of the Origin, Evolution and Dispersal of the Late Pleistocene* Mammuthus-Coelodonta *Faunal Complex in Eurasia (Large Mammals)*. Mammoth Site of Hot Springs, SD. Inc., Rapid City, South Dakota.

Komatsu, G., Baker, V.R., Arzhannikov, S.G., Gallagher, R., Arzhannikova, A.V., Murana, A., Oguchi, T., 2016. Catastrophic flooding, palaeolakes, and late Quaternary drainage reorganization in northern Eurasia. *International Geology Review* **58**, 1693–1722.

Kovalskiy, V.V., 1974. *Geokhimicheskaya Ekologiya*. Nauka, Moskwa. [in Russian]

Krivonogov, S.K., Gusev, V.A., Parkhomchuk, E.V., Zhilich, S.V., 2018. Intermediate lakes of the Chulym and Kargat river valleys and their role in the evolution of the Lake Chany basin. *Russian Geology and Geophysics* **59**, 541–555.

Krzemińska, A., 2014. *Abnormalities and Other Changes on Woolly Mammoth Bones from Central Europe 32,000 to 20,000 Years Ago—A Monograph*. Faunistic Monographs 27. Instytut Systematyki i Ewolucji Zwierząt, Polska Akademia Nauk, Kraków.

Krzemińska A., Wędzicha S., 2015. Pathological changes on the ribs of woolly mammoths (*Mammuthus primigenius*). *Quaternary International* 359–360, 186–194.

Krzemińska, A., Wojtal, P., Oliva, M., 2015. Pathological changes on woolly mammoth (*Mammuthus primigenius*) bones: holes, hollows and other minor changes in the spinous processes of vertebrae. *Quaternary International* 359–360, 178–185.

Kuitems, M., van Kolfschoten, T., Tikhonov, A.N., van der Plicht, J., 2019. Woolly mammoth $\delta^{13}C$ and $\delta^{15}N$ values remained amazingly stable throughout the last ~50,000 years in north-eastern Siberia. *Quaternary International* **500**, 120–127.

Kuzmin, Y.V., 2010. Extinction of the woolly mammoth (*Mammuthus primigenius*) and woolly rhinoceros (*Coelodonta antiquitatis*) in Eurasia: review of chronological and environmental issues. *Boreas* **39**, 247–261.

Kuzmin, Y.V., Bondarev, A.A., Kosintsev, P.A., Zazovskaya, E.P., 2021. The Paleolithic diet of Siberia and Eastern Europe: evidence based on stable isotopes ($\delta^{13}C$ and $\delta^{15}N$) in hominin and animal bone collagen. *Archaeological and Anthropological Sciences* **13**, 179. https://doi.org/10.1007/s12520-021-01439-5.

Kuzmina, I.E., Maschenko, E.N., 1999. Age morphological changes in the skull and skeleton of mammoth calves of the Russia Plane. In: Kuzmina, I.E. (Ed.), *Mammoth Calves* Mammuthus primigenius *(Blumenbach, 1799)*. Chapter 3, Proceedings of the Zoological Institute 275, Russian Academy of Sciences, St. Petersburg, pp. 51–120. [in Russian]

Lang, E.M., 1980. Observations on growth and molar change in the African elephant. *African Journal of Ecology* **18**, 217–234.

Larramendi, A. 2016. Shoulder height, body mass, and shape of proboscideans. *Acta Palaeontologica Polonica* **61**, 537–574.

Laws, R.M., 1966. Age criteria for the African elephant, *Loxodonta a. africana*. *East African Wildlife Journal* **4**, 1–37.

Lee, Ph.C., Sayialel, S., Lindsay, W.K., Moss, C.J., 2012. African elephant age determination from teeth: validation from known individuals. *African Journal of Ecology* **50**, 9–20.

Leshchinskiy, S.V., 2001. Late Pleistocene beast solonetz of Western Siberia: «mineral oases» in mammoth migration paths, foci of the Palaeolithic man's activity. In: Cavarretta, G., Gioia, P., Mussi, M., Palombo, M.R. (Eds), *The World of Elephants*. Proceedings of the 1st International Congress, October 16–20. CNR, Rome, pp. 293–298.

Leshchinskiy, S.V., 2006. Lugovskoye: environment, taphonomy, and origin of a paleofaunal site. *Archaeology, Ethnology & Anthropology of Eurasia* **25**, 33–40.

Leshchinskiy, S.V., 2009. Mineral deficiency, enzootic diseases and extinction of mammoth of Northern Eurasia. *Doklady Biological Sciences* **424**, 72–74.

Leshchinskiy, S.V., 2012. Paleoecological investigation of mammoth remains from the Kraków Spadzista Street (B) site. *Quaternary International* 276–277, 155–169.

Leshchinskiy, S., 2015. Enzootic diseases and extinction of mammoths as a reflection of deep geochemical changes in ecosystems of Northern Eurasia. *Archaeological and Anthropological Sciences* **7**, 297–317.

Leshchinskiy, S.V., 2017. Strong evidence for dietary mineral imbalance as the cause of osteodystrophy in Late Glacial woolly mammoths at the Berelyokh site (Northern Yakutia, Russia). *Quaternary International* **445**, 146–170.

Leshchinskiy, S.V., Maschenko, E.N., Ponomareva, E.A., Orlova, L.A., Burkanova, E.M., Konovalova, V.A., Teterina I.I., Gevlya, K.M., 2006. Multidisciplinary paleontological and stratigraphic studies at Lugovskoe (2002–2004). *Archaeology, Ethnology & Anthropology of Eurasia* **25**, 54–69.

Leshchinskiy, S.V., Kuzmin, Y.V., Zenin, V.N., Jull, A.J.T., 2008. Radiocarbon chronology of the "Mammoth Cemetery" and Paleolithic site of Volchia Griva (Western Siberia). *Current Research in the Pleistocene* **25**, 53–56.

Leshchinskiy, S.V., Zenin, V.N., Burkanova, E.M., Dudko, A.A., Gulina, A.V., Fedyaev, N.Ya., Semiryakov, A.S., Kanishcheva, E.V., 2015. Multidisciplinary studies of the Baraba mammoth refugium in 2015. *Tomsk State University Journal* **400**, 354–365. [in Russian]

Leshchinskiy, S.V., Kuzmin, Y.V., Boudin, M., Amon, L., 2021a. Holes in the spinous processes of woolly mammoth vertebrae: spatial and temporal distribution, and the causes of pathology formation. *Journal of Quaternary Science* **36**, 1254–1267.

Leshchinskiy, S.V., Zenin, V.N., Bukharova, O.V., 2021b. The Volchia Griva mammoth site as a key area for geoarchaeological research of human movements in the Late Paleolithic of the West Siberian Plain. *Quaternary International* 587–588, 368–383.

Levina, T.P., Orlova, L.A., 1993. Holocene climatic rhythms of southern West Siberia. *Geologiya i Geofizika* **34**, 36–51. [in Russian]

Liss, O.L., Abramova, L.I., Avetov, N.A., Berezina, N.A., Inisheva, L.I., Kurnushkova, T.V., Sluka, Z.A., Tolpysheva, T.Yu., Shvedchikova, N.K., 2001. *Bolotnye Sistemy Zapadnoy Sibiri i ih Prirodoohrannoe Znachenie*. Izdatelstvo Grif i K, Tula.

Lister, A.M., 1999. Epiphyseal fusion and postcranial age determination in the woolly mammoth *Mammuthus primigenius*. *Deinsea* **6**, 79–87.

Logginov, A., 1890. *K voprosu ob osteoporoze, kak samostoyatelnoi bolezni u loshadei*. Veterinary Dissertation. Tipografiya G. Lakmana, Derpt. [in Russian]

Mangerud, J., Jakobsson, M., Alexanderson, H., Astakhov, V., Clarke, G.K.C., Henriksen, M., Hjort, C., *et al.*, 2004. Ice-dammed lakes and rerouting of the drainage of northern Eurasia during the Last Glaciation. *Quaternary Science Reviews* **23**, 1313–1332.

Maschenko, E.N., 2002. Individual development, biology and evolution of the woolly mammoth. *Cranium* **19**, 4–120.

Mashchenko, E.N., Leshchinskiy, S.V., 2001. Composition and morphology of mammoth remains from the Volchia Griva site. In: Podobina, V.M. (Ed.), *Evolution of Life on the Earth*: Proceedings of the II International Symposium. Tomsk State University, Tomsk, pp. 507–511. [in Russian]

Mwangi, P.N., Milewski, A., Wahungu, G.M., 2004. Chemical composition of mineral licks used by elephants in Aber-dares National Park, Kenya. *Pachyderm* **37**, 59–67.

Nadachowski, A., Lipecki, G., Wojtal, P., Miękina, B., 2011. Radiocarbon chronology of woolly mammoth (*Mammuthus primigenius*) from Poland. *Quaternary International* **245**, 186–192.

Nadachowski, A., Lipecki, G., Baca, M., Żmihorski, M., Wilczyński, J., 2018. Impact of climate and humans on the range dynamics of the woolly mammoth (*Mammuthus primigenius*) in Europe during MIS 2. *Quaternary Research* **90**, 439–456.

Okladnikov, A.P., Grigorenko, B.G., Alexeeva, E.V., Volkov, I.A. 1971. Stoyanka verhnepaleoliticheskogo cheloveka Volchia Griva (raskopki 1968 goda). *Materialy polevyh issledovaniy Dal'nevostochnoi arheologicheskoy ekspedicii* 2. NII IFF SO AN SSSR, Novosibirsk, pp. 87–131. [in Russian]

Orlova, L.A., 1990. *Golocen Baraby (Stratigrafiya i Radiouglerodnaya Chronologiya)*. Nauka, Sibirskoe Otdelenie, Novosibirsk. [in Russian]

Perelman, A.I., 1975. *Geohimiya Landshafta*. Vysshaya Shkola, Moskva. [in Russian]

Petrov, B.F., 1948. Proishozhdenie rel'efa Baraby. *Bulleten' komissii po izucheniyu chetvertichnogo perioda* **12**, 93–97. [in Russian]

Pogoda i klimat, 2020. *Spravochno-informacionnyi portal*. http://www.pogodaiklimat.ru/ (accessed 10 June 2020).

Polunin, G.V., 1961. O krupnom zahoronenii mamontov v Barabinskoy stepi. *Trudy SNIIGGiMS* **14**, 46–48. [in Russian]

Puzachenko, A.Yu., Markova, A.K., Kosintsev, P.A., van Kolfschoten, T., van der Plicht, J., Kuznetsova, T.V., Tikhonov, A.N., Ponomarev, D.V., Kuitems, M., Bachura, O.P., 2017. The Eurasian mammoth distribution during the second half of the Late Pleistocene and the Holocene: regional aspects. *Quaternary International* **445**, 71–88.

Rabanus-Wallace, M.T., Wooller, M.J., Zazula, G.D., Shute, E., Jahren, A.H., Kosintsev, P., Burns, J.A., Breen, J., Llamas, B., Cooper, A., 2017. Megafaunal isotopes reveal role of increased moisture on rangeland during late Pleistocene extinctions. *Nature Ecology & Evolution* **1**, 0125. https://doi.org/10.1038/s41559-017-0125.

Reineck, H.-E., Singh, I.B., 1975. *Depositional Sedimentary Environments (with reference to terrigenous clastics)*. Corrected reprint of the first ed. Springer-Verlag, Berlin, Heidelberg, New York.

Roth, V.L., Shoshani, J., 1988. Dental identification and age determination in *Elephas maximus*. *Journal of the Zoological Society of London* **214**, 567–588.

Rothschild, B.M., Laub, R., 2006. Hyperdisease in the Late Pleistocene: validation of an early 20th century hypothesis. *Naturwissenschaften* **93**, 557–564.

Rothschild, B.M., Laub, R., 2008. Pedal stress fractures in mastodons. *Journal of Paleopathology* **20**, 43–51.

Rothschild, B.M., Martin, L.D., 2003. Frequency of pathology in a large natural sample from Natural Trap Cave with special remarks on erosive disease in the Pleistocene. *Reumatismo* **55**, 58–65.

Rothschild, B.M., Wang, X., Shoshani, J., 1994. Spondyloarthropathy in Proboscideans. *Journal of Zoo and Wildlife Medicine* **25**, 360–366.

Rountrey, A.N., Fisher, D.C., Tikhonov, A.N., Kosintsev, P.A., Lazarev, P.A., Boeskorov, G., Buigues, B., 2012. Early tooth development, gestation, and season of birth in mammoths. *Quaternary International* **255**, 196–205.

Seuru, S., Leshchinskiy, S., Auguste, P., Fedyaev, N., 2017. Woolly mammoth and man at Krasnoyarskaya Kurya site, West Siberian plain, Russia (excavation results of 2014). *Bulletin de la Societe Geologique de France* **188**, 1–13.

Shpansky, A.V., 2014. Variations of the tooth morphology of the woolly mammoth *Mammuthus primigenius* (Blumenbach, 1799) (Mammalia: Elephanthidae). *Proceedings of the Zoological Institute RAS* **318**, 24–33. [in Russian]

Shrock, R.R., 1948. *Sequence in Layered Rocks*. First ed. (second impression). McGraw-Hill, New York, Toronto, London.

Shvartsev, S.L., 1992. O sootnoshenii sostavov podzemnyh vod i gornyh porod. *Geologia i Geofizika* **8**, 46–55. [in Russian]

Shvartsev, S.L., 1998. *Gidrogeohimiya Zony Gipergeneza*. Nedra, Moskva. [in Russian]

Stuart, A.J., Sulerzhitsky, L.D., Orlova, L.A., Kuzmin, Y.V., Lister, A.M., 2002. The latest woolly mammoths (*Mammuthus primigenius* Blumenbach) in Europe and Asia: a review of the current evidence. *Quaternary Science Reviews* **21**, 1559–1569.

Stuart, A.J., Kosintsev, P.A., Higham, T.F.G., Lister, A.M., 2004. Pleistocene to Holocene extinction dynamics in giant deer and wooly mammoth. *Nature* **431**, 684–689.

Sulerzhitsky, L.D., Romanenko, F.A., 1997. Age and distribution of the "mammoth" fauna of the polar region of Asia (radiocarbon dating results). *Earth Cryosphere* **1**, 12–19. [in Russian]

Szpak, P., Gröcke, D.R., Debruyne, R., MacPhee, R.D.E., Guthrie, R.D., Froese, D., Zazula, G.D., Patterson, W.P., Poinar, H.N., 2010. Regional differences in bone collagen $\delta^{13}C$ and $\delta^{15}N$ of Pleistocene mammoths: implications for paleoecology of the mammoth steppe. *Palaeogeography, Palaeoclimatology, Palaeoecology* **286**, 88–96.

Tarasov, P.E., 2000. Rekonstrukciya climata i rastitelnosti Severnoy Evrazii pozdnego pleistocena po palinilogicheskim dannym. In: Kaplin, P.A., Sudakova, N.G. (Eds.), *Problemy Paleogeografii i Stratigrafii Pleistocena*. Izdatelstvo Moskovskogo Universiteta, Moskva, pp. 70–96. [in Russian]

Ukkonen, P., Aaris-Sørensen, K., Arppe, L., Clark, P.U., Daugnora, L., Lister, A.M., Lõugas, L., *et al.*, 2011. Woolly mammoth (*Mammuthus primigenius* Blum.) and its environment in northern Europe during the last glaciation. *Quaternary Science Reviews* **30**, 693–712.

van der Plicht, J., Molodin, V.I., Kuzmin, Y.V., Vasiliev, S.K., Postnov, A.V., Slavinsky, V.S., 2015. New Holocene refugia of giant deer (*Megaloceros giganteus* Blum.) in Siberia: updated extinction patterns. *Quaternary Science Reviews* **114**, 182–188.

Vartanyan, S.L., Arslanov, Kh.A., Tertychnaya, T.V., Chernov, S.B., 1995. Radiocarbon dating evidence for mammoths on Wrangel Island, Arctic Ocean, until 2000 BC. *Radiocarbon* **37**, 1–6.

Velichko, A.A., Timireva, S.N., Kremenetski, K.V., MacDonald, G.M., Smith, L.C., 2011. West Siberian Plain as a late glacial desert. *Quaternary International* **237**, 45–53.

Vereshchagin, N.K., 1977. Berelyokhskoe "kladbishche" mamontov. In: Starobogatov, Ja.I. (Ed), Mamontovaya fauna Russkoy ravniny i Vostochnoy Sibiri. *Academy of Sciences of the USSR, Leningrad, Proceedings of the Zoological Institute* 72, 5–50. [in Russian]

Vogel, J.S., Southon, J.R., Nelson, D.E., Brown, T.A., 1984. Performance of catalytically condensed carbon for use in accelerator mass spectrometry. *Nuclear Instruments and Methods in Physics Research B* **5**, 289–293.

Volkova, V.S., Mikhailova, I.V., 2001. Environment and climate in the Last (Sartan) Glaciation in West Siberia (according to palynological evidence). *Geologiya i Geofizika* **42**, 678–689. [in Russian]

Walker, D.A., Bockheim, J.G., Chapin, F.S., III, Eugster, W., Nelson, F.E., Ping, C.L., 2001. Calcium-rich tundra, wildlife, and the "Mammoth Steppe". *Quaternary Science Reviews* **20**, 149–163.

Wißing, C., Rougier, H., Baumann, C., Comeyne, A., Crevecoeur, I., Drucker, D.G., Gaudzinski-Windheuser, S., *et al.*, 2019. Stable isotopes reveal patterns of diet and mobility in the last Neandertals and first modern humans in Europe. *Scientific Reports* **9**, 4433. https://doi.org/10.1038/s41598-019-41033-3.

Zaklinskaya, E.D., Panova, L.A. (Eds.), 1986. *Metodicheskiye Rekomendacii k Tehnike Obrabotki Osadochnyh Porod pri Sporovo-Pylcevom Analize*. Ministerstvo geologii SSSR, VSEGEI, Leningrad. [in Russian]

Zenin, V.N., 2002. Major stages in the human occupation of the West Siberian Plain during the Paleolithic. *Archaeology, Ethnology & Anthropology of Eurasia* **4**, 22–44.

Zenin, V.N., Leshchinskiy, S.V., Zolotarev, K.V., Grootes, P.M., Nadeau, M.-J., 2006. Lugovskoe: geoarchaeology and culture of a Paleolithic site. *Archaeology, Ethnology & Anthropology of Eurasia* **25**, 41–53.

Zhylkibaev, K.Zh., 1963. Iskopaemye ostatki slonov v kollekciyah Instituta zoologii AN KazSSR. *Materialy po istorii fauny i flory Kazahstana* IV, 66–76. [in Russian]

Zykin, V.S., Zykina, V.S., 2009. Problems of subdivision and correlation of the Quaternary deposits in the southern West Siberian plain. *Bulletin of Commission for study of the Quaternary* **69**, 71–84. [in Russian]

Zykin, V.S., Zykina, V.S., Orlova, L.A., 2002. Novye dannye ob izmenenii prirodnoi sredy i klimata v pozdnem Pleistocene yuga Zapadno-Sibirskoy ravniny po osadkam kotloviny ozera Aksor. In: Vaganov, E.A., Derevianko, A.P., Grachev, M.A., Zykin, V.S., Markin, S.V. (Eds.), *Osnovnye Zakonomernosti Globalnyh i Regionalnyh Izmeneniy Klimata i Prirodnoy Sredy v Pozdnem Kaynozoe Sibiri*. Izdatelstvo IAE SO RAN, Novosibirsk, pp. 220–233. [in Russian]